WILEY-BLACKWELL

Cladistics (2021) 1–25

Cladistics

10.1111/cla.12480

Diversity, host specificity and biogeography in the Cladocorynidae (Hydrozoa, Capitata), with description of a new genus

Davide Maggioni[a,b]*, Agustín Garese[c], Danwei Huang[d], Bert W. Hoeksema[e,f], Roberto Arrigoni[g], Davide Seveso[a,b], Paolo Galli[a,b], Michael L. Berumen[h], Enrico Montalbetti[a,b], Daniela Pica[i,j], Fabrizio Torsani[k] and Simone Montano[a,b]

[a]*Department of Earth and Environmental Sciences (DISAT), University of Milano-Bicocca, Piazza della Scienza, Milano, 20126, Italy;* [b]*Marine Research and High Education (MaRHE) Center, University of Milano-Bicocca, Faafu Magoodhoo Island, 12030, Republic of Maldives;* [c]*Instituto de Investigaciones Marinas y Costeras (IIMyC), Facultad de Ciencias Exactas y Naturales, Universidad Nacional de Mar del Plata (UNMDP) – Consejo Nacional de Investigaciones Científicas y Técnicas (CONICET), Mar del Plata, 7600, Argentina;* [d]*Department of Biological Sciences, Tropical Marine Science Institute and Centre for Nature-based Climate Solutions, National University of Singapore, Singapore, 117558, Singapore;* [e]*Taxonomy, Systematics and Geodiversity Group, Naturalis Biodiversity Center, Leiden, 2300 RA, The Netherlands;* [f]*Groningen Institute for Evolutionary Life Sciences, University of Groningen, Groningen, 9700 CC, The Netherlands;* [g]*Department of Biology and Evolution of Marine Organisms (BEOM), Stazione Zoologica Anton Dohrn, Villa Comunale, Napoli, 80121, Italy;* [h]*Red Sea Research Center, Division of Biological and Environmental Science and Engineering, King Abdullah University of Science and Technology (KAUST), Thuwal, 23955-6900, Saudi Arabia;* [i]*Department of Biological and Environmental Sciences and Technologies, University of Salento, Lecce, 73100, Italy;* [j]*CoNISMa – Consorzio Nazionale Interuniversitario per le Scienze del Mare, Roma, 00196, Italy;* [k]*Department of Life and Environmental Sciences, Polytechnic University of Marche, Ancona, 60131, Italy*

Accepted 17 June 2021

Abstract

The hydrozoan family Cladocorynidae inhabits tropical to temperate waters and comprises the two genera *Pteroclava* and *Cladocoryne*. *Pteroclava* lives in association with some octocorals and hydrozoans, whereas *Cladocoryne* is more generalist in terms of substrate choice. This work provides a thorough morpho-molecular reassessment of the Cladocorynidae by presenting the first well-supported phylogeny of the family based on the analyses of three mitochondrial and four nuclear markers. Notably, the two nominal genera were confirmed to be monophyletic and both morphological and genetic data led to the formal description of a new genus exclusively associated with octocorals, *Pseudozanclea* gen. nov. Maggioni & Montano. Accordingly, the diagnosis of the family was updated. The ancestral state reconstruction of selected characters revealed that the symbiosis with octocorals likely appeared in the most recent common ancestor of *Pteroclava* and *Pseudozanclea*. Additionally, the presence of euryteles aggregation in the polyp stage and the exumbrellar nematocyst pouches with euryteles represent synapomorphies of all cladocorynid taxa and probably emerged in their most recent common ancestor. The analysis of several *Pteroclava krempfi* colonies from Indo-Pacific and Caribbean localities associated with several host octocorals revealed a high intra-specific genetic variability. Single- and multi-locus species delimitations resulted in three to five species hypotheses, but the statistical analysis of morphometric data showed only limited distinction among the clades of *P. krempfi*. However, *P. krempfi* clades showed differences in both host specificity, mostly at the octocoral family level, and geographic distribution, with one clade found exclusively in the Caribbean Sea and the others found in the Indo-Pacific.

*Corresponding author:
E-mail address: davide.maggioni@unimib.it

Introduction

Coral reefs are well known to host a great diversity of symbiotic relations, with scleractinian corals being associated with numerous other organisms, spanning all domains of life (Gates and Ainsworth, 2011; Stella et al., 2011; Hoeksema et al., 2012, 2017). Coral associates may interact with each other and the host, resulting in positive outcomes for the whole coral symbiome (Ainsworth et al., 2020), but in many cases these interactions are still poorly characterized, in particular for their taxonomic composition and ecological relevance (Gates and Ainsworth, 2011). Other benthic coral-reef invertebrates also provide habitats for a plethora of organisms (e.g., Antokhina and Britayev, 2012; Neo et al., 2015; Schönberg et al., 2015; García-Hernández et al., 2019), even if these associations are rarely well characterized (Montano, 2020).

Octocorals represent a prominent group among non-scleractinian reef dwellers (Fabricius and Alderslade, 2001), and, due to their topological complexity and abundance, they host several associated organisms (Goh et al., 1999; Hoeksema et al., 2015). For instance, Maggioni et al., (2020a) recently reported the octocoral *Bebryce* cf. *grandicalyx* to recurrently host the hydroid *Zanclea timida* Puce, Di Camillo and Bavestrello, 2008 together with a suberitid sponge in the Maldives, and many other invertebrates were observed to dwell on the octocoral or sponge surface. This octocoral-hydrozoan symbiosis is not an exception, as many hydrozoan and octocoral species are reported to live in intimate associations (Bo et al., 2011). Some of these hydroids appear to be obligate symbionts of octocorals and have never been reported growing on other substrates (Puce et al., 2008a, b).

The aforementioned *Z. timida*, and the cladocorynid *Pteroclava krempfi* (Billard, 1919) are two examples of obligate alcyonancean-associated hydrozoan species (Puce et al., 2008b). Both species are known to grow on a variety of hosts: *Z. timida* is associated with the alcyonacean genera *Paratelesto* Utinomi, 1958 and *Bebryce* Philippi, 1841 (Puce et al., 2008b; Maggioni et al., 2020a), whereas *P. krempfi* associates with at least nine alcyonacean genera (Billard, 1919; Varela and Cabrales Caballero, 2010; Seveso et al., 2016, 2020; Maggioni et al., 2016; Montano et al., 2017). Genetic data of *P. krempfi* have revealed the presence of a complex of multiple cryptic species with a possible host specificity at the octocoral genus or family level (Maggioni et al., 2016; Montano et al., 2017). Specifically, a Maldivian clade was associated with *Paraplexaura* Kükenthal, 1909 (family Plexauridae Gray, 1859), a second Maldivian clade was found exclusively on the Alcyoniidae Lamouroux, 1812 genera *Sinularia* May, 1898, *Sarcophyton* Lesson, 1834, and *Lobophytum* Marenzeller, 1886, whereas a third Caribbean clade was associated with *Antillogorgia* Bayer, 1951 (family Gorgoniidae Lamouroux, 1812). Despite the host preferences and genetic divergence, no morphological differences were detected among the three *P. krempfi* clades. This, along with (i) the lack of suitable genetic material of *P. krempfi* from the type locality (in Vietnam), and (ii) the type's host *Cladiella krempfi* (Hickson, 1919) and (iii) the scant information on the congeneric and hydrozoan-associated species *Pteroclava crassa* (Pictet, 1893), did not allow the authors to name the species.

Taxonomic confusion is also evident in the other cladocoryinid genus, *Cladocoryne* Rotch, 1871. All *Cladocoryne* species are characterized by the unique aboral branched tentacles (Bouillon et al., 2006), and the number and arrangement of aboral tentacles are key distinguishing characters for the species of this genus (Schuchert, 2003). This taxon currently contains five species, three of which [*Cladocoryne travancorensis* (Mammen, 1963), *Cladocoryne littoralis* (Mammen, 1963), *Cladocoryne minuta* Watson, 2005] have never been observed again after their first description (Mammen, 1963; Watson, 2005). The other two well-established species, namely *Cladocoryne floccosa* Rotch, 1871 and *Cladocoryne haddoni* Kirkpatrick, 1890, can be easily distinguished by the number of aboral branched tentacles and the cnidome (Bouillon et al., 1987). The presence of unnamed *Cladocoryne* species has also been hypothesized by Schuchert (2003) while discussing Indonesian colonies described by Stechow and Müller (1923) and Vervoort (1941), yet no molecular analyses have been performed to assess the precise diversity of the genus. Moreover, the type material of *C. floccosa*, *C. travancorensis*, and *C. littoralis* cannot currently be located, and is presumably lost.

In contrast to *Pteroclava* Weill, 1931, the genus *Cladocoryne* is a generalist in terms of substrate choice, and has been reported on a variety of substrates, including rocks, algae, seagrasses, sponges, octocorals, bryozoans, polychaete tubes, and other hydroids (Bouillon et al., 1987; Gravili et al., 2015). Additional differences are found in the general morphology and reproductive structures, since *Pteroclava* has moniliform tentacles and produces free-swimming medusae, whereas *Cladocoryne* has oral capitate and aboral branched capitate tentacles and produces cryptomedusoids that do not detach from the parental polyp (Bouillon et al., 2006). However, both genera share the presence of euryteles grouped in rounded clusters in the polyp stage, a feature considered to be a synapomorphy of taxa ascribed to Cladocorynidae Allman, 1872 (Petersen, 1990). Other unique features of the family are (i) the presence of euryteles in the exumbrellar cnidocyst pouches, occurring in the free-swimming medusa of *P. krempfi* (Boero et al., 1995),

and (ii) the branched aboral tentacles in all *Cladocoryne* species (Bouillon et al., 2006).

With this work we aimed at performing a thorough assessment of the family Cladocorynidae, including detailed morphological characterisations, phylogenetic analyses, single and multi-locus DNA-based species delimitations, statistics of morphological measurements, character evolution, and host-specificity assessment. Additionally, the phylogenetic position of the octocoral-associated species *Zanclea timida* was assessed based on new morphological information (i.e., the medusa stage) and genetic data.

Material and methods

Sampling and morphological assessment

Sampling was carried out by snorkelling (0–5 m deep) and diving (5–30 m deep) between November 2013 and November 2018 in several localities across the Indo-Pacific, Red Sea, Caribbean Sea, and Mediterranean Sea (Fig. 1, Table S1). All species were collected in this depth range, with the only exception of *Zanclea timida* colonies at 40–50 m depth. When the presence of hydrozoan polyps was recorded *in situ*, small fragments of the substrate and associated hydroids were collected. Animals were anesthetized with menthol crystals, detached from their hosts using precision forceps, hypodermic syringe needles, and micropipettes and subsequently fixed in both 99% ethanol for molecular analyses and 10% formalin for morphological analyses. When possible, live animals were reared in constantly oxygenated bowls filled with seawater, at room temperature, under artificial light, and fed with *Artemia* nauplii until medusa release occurred.

Hydrozoans were identified to the species level following Boero et al., (1995), Bouillon et al., (1987), Schuchert (2006), and Puce et al., (2008). Cladocorynid specimens were observed and photographed under a Leica EZ4 D stereo microscope to assess their general morphology, and analyzed under a Zeiss Axioskop 40 compound microscope to study the fine-scale morphology of polyps, medusae, and cnidocysts. All measurements were taken using ImageJ 1.52p software. For the identification of host octocorals, small portions of tissue were immersed in a 10% sodium hypochlorite solution for 6 h to obtain sclerites. Octocorals were identified to genus level or, when possible, to the species level by examining the general morphology of the colony and the sclerites following Fabricius and Alderslade (2001) and Williams and Chen (2012).

New material for each investigated species was deposited at the Museo Civico di Storia Naturale di Milano (Italy) and the Australian Museum (Sydney, Australia). The present work is registered in ZooBank under: http://zoobank.org/urn:lsid:zoobank.org:pub:EED5AABF-43CC-4793-A84E-3C49857D33B8.

DNA extraction and sequencing

Total genomic DNA was extracted from ethanol-fixed hydroids using the protocol described in Maggioni et al., (2020b). Additional DNA samples of *Cladocoryne floccosa* colonies from the Caribbean and Mediterranean Sea were obtained from Peter Schuchert (Muséum d'Histoire Naturelle of Geneva, Switzerland, Table S1).

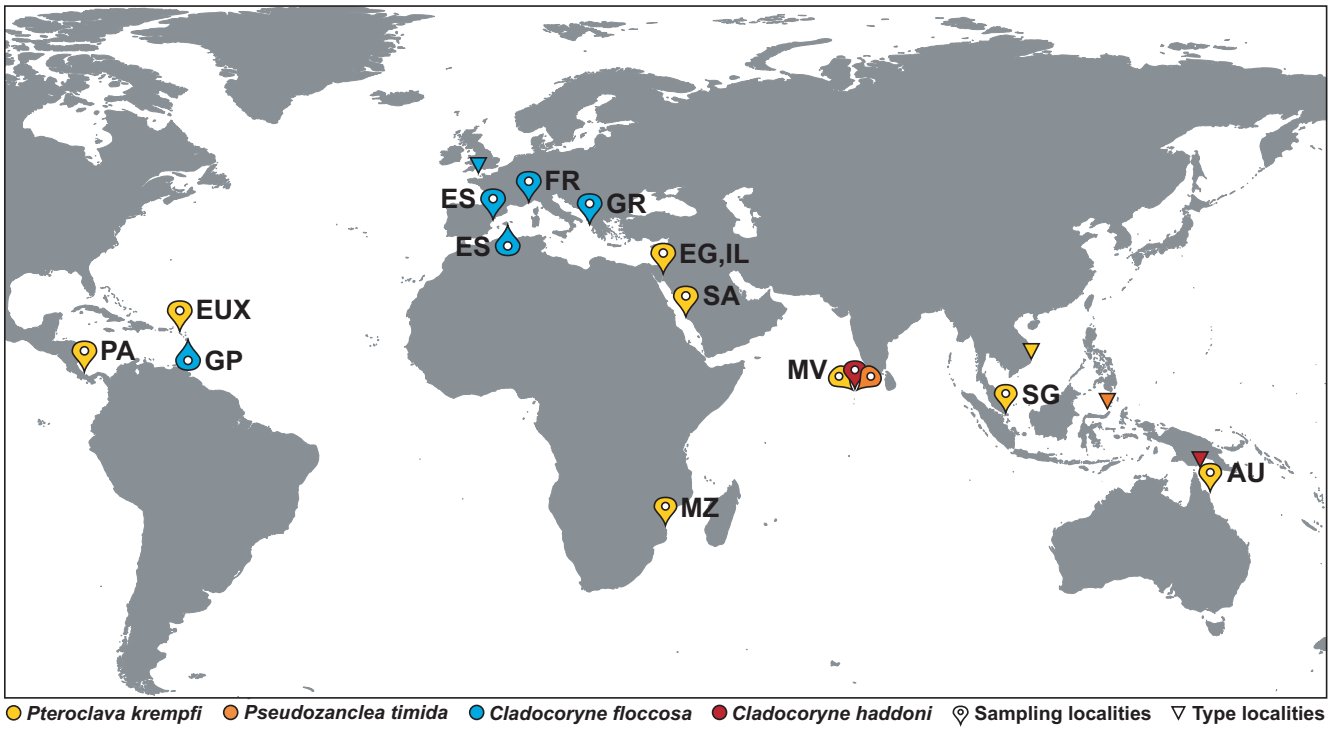

Fig. 1. Map of the sampling sites. Triangles show type localities of the investigated species, whereas pins show sampling localities, coloured by species, as shown in the legend. Caribbean Sea: GP, Guadeloupe; PA, Panama; EUX, St. Eustatius. Mediterranean Sea: ES, Spain; FR, France; GR, Greece. Red Sea: EG, Egypt; IL, Israel; SA, Saudi Arabia. Indo-West Pacific: AU, Australia; MV, Maldives; MZ, Mozambique; SG, Singapore.

Table 1
Molecular statistics and substitution models for each molecular markers

Region	Primers	S	Sv (%)	SPI (%)	H	Hd	Nd	Substitution models
16S rRNA	SHB-SHA	625	157 (25.1)	123 (19.7)	55	0.973 ± 0.008	0.100 ± 0.007	HKY + I + G
COX1	LCO1490-HCO2198	677	187 (27.6)	167 (24.7)	52	0.976 ± 0.009	0.131 ± 0.006	HKY + I + G
COX3	CO3F-CO3R	668	264 (39.5)	233 (34.9)	65	0.990 ± 0.004	0.150 ± 0.008	GTR + I + G
18S rRNA	18SA-18SB	1712	185 (10.8)	109 (6.4)	29	0.910 ± 0.016	0.012 ± 0.002	GTR + I + G
28S rRNA	28SHF-R2077	1684	250 (14.8)	165 (9.8)	25	0.831 ± 0.030	0.022 ± 0.002	GTR + I + G
ITS (Gblocks)	HITSF-HITSR	662	191 (28.9)	133 (20.1)	21	0.809 ± 0.031	0.074 ± 0.011	GTR + I + G
H3	H3F-H3R	352	68 (19.3)	56 (15.9)	22	0.873 ± 0.023	0.091 ± 0.009	GTR + G

H, number of unique haplotypes; Hd, haplotype diversity; Nd, nucleotide diversity; S, number of sites; SPI, number of parsimony-informative sites; Sv, number of variable sites.

Seven gene regions were amplified using the primers and protocols described in Maggioni et al., (2020c), namely portions of the mitochondrial large ribosomal RNA (16S rRNA), cytochrome oxidase subunit I (COX1), cytochrome oxidase subunit III (COX3), and nuclear small ribosomal RNA (18S rRNA), large ribosomal RNA (28S rRNA), internal transcribed spacer (ITS; including partial ITS1, 5.8S, and partial ITS2 regions), and histone H3 (H3) (Table 1). PCR products were checked through 1.5% agarose electrophoretic runs, purified with Illustra ExoStar (GE Healthcare: Amersham, UK) and sequenced in both directions with ABI 3730xl DNA Analyzer (Applied Biosystems: Carlsbad, CA, USA). Geneious 6.1.6 was used to visually check, correct, and assemble the obtained chromatograms and to check for the presence of open reading frames in protein-coding genes. The consensus sequences obtained in this study were deposited in GenBank with the accession numbers listed in Table S1.

Sequences of each DNA region were aligned using MAFFT 7.110 (Katoh and Standley, 2013) with the E-INS-i option, after adding outgroup sequences following Maggioni et al., (2017, 2018) (Tables S1). The ITS alignment was further run through Gblocks (Castresana, 2000; Talavera and Castresana, 2007) using the default 'less stringent' settings to remove ambiguously aligned regions. All alignments were also concatenated using Mesquite 3.2 (Maddison and Maddison, 2006).

Phylogenetic analyses

Descriptive statistics and variability of each DNA region were calculated with DnaSP 6 (Rozas et al., 2017) (Table 1). Substitution models were determined using jModelTest 2 (Darriba et al., 2012) for single-locus datasets, whereas partition schemes and models were determined with PartitionFinder 1.1.1 (Lanfear et al., 2012) for the multi-locus dataset (Table S2), using the Akaike Information Criterion (AIC).

Phylogenetic inference was performed using maximum parsimony (MP), maximum likelihood (ML), and Bayesian inference (BI) using both single- and multi-locus datasets and running the analyses on the CIPRES server (Miller et al., 2010). MP analyses were performed using PAUP 4.0b10 (Swofford, 2003) with heuristic searches stepwise addition and tree-bisection-reconnection branch swapping. Node support was assessed using 1000 bootstrap replicates with randomly added taxa. For ML analyses, the substitution model GTR+G was selected for each DNA region and partition, and analyses were run using RAxML 8.2.12 (Stamatakis, 2014) with 1000 non-parametric bootstrap replicates. BI analyses were performed using MrBayes 3.2.6 (Ronquist et al., 2012) using the substitution models and partitions listed in Table S2. Two independent runs for four Markov chains were conducted for 50 million generations, with trees sampled every 5000th generation. For all Bayesian analyses, parameter estimates and convergence were checked using Tracer 1.6 (Rambaut et al., 2014), where burn-in was set at 25%.

MEGA X (Kumar et al., 2018) was used to calculate genetic distances within and among the obtained clades. Genetic distances were calculated as % uncorrected *p*-distances with 1000 non-parametric bootstrap replicates.

A species tree was obtained using *BEAST (Heled and Drummond, 2009) in BEAST 2.2.0 (Bouckaert et al., 2014). Specimens were assigned to different species according to the species delimitation analyses described below, and mitochondrial loci were considered as a single partition, whereas nuclear loci were kept separate. Yule process prior, together with a linear and constant-root population-size model, were used and each analysis was run for 10^8 generations, sampling every 10000th generation, and setting a 25% burn-in. The convergence of the analysis was checked using Tracer 1.6 (Rambaut et al., 2014), as done for the gene trees.

To better visualize the presence of host-related and geography-related genetic structure within *Pteroclava* clades, median-joining haplotype networks were built using the software PopART 1.7 (Leigh and Bryant, 2015). The most complete mitochondrial single-locus dataset (16S rRNA) was used, with haplotypes coloured according to the genus of the host and the geographic provenance (Indian Ocean, Pacific Ocean, Red Sea).

Finally, a set of characters was mapped onto a reduced multi-locus phylogenetic reconstruction of the Zancleida Russel, 1953 (including one specimen for each nominal species) obtained with BEAST 1.8.2 (Drummond et al., 2012) using the same parameters described for the *BEAST analysis. The mapped characters were: (i) the organisation of euryteles in the polyp stage (not organized, organized in clusters or a ring); (ii) the exumbrellar cnidocyst pouches in the medusa stage (absent, containing euryteles, containing stenoteles); (iii) the substrate choice of the polyp stage (generalist, symbiotic); (iv) the host of the polyp stage (none, octocorals, sponges, scleractinians, bryozoans). Stochastic mapping (Huelsenbeck et al., 2003) was used to map probable realizations of the evolution of the considered characters on the Zancleida tree. The analyses were run in the R environment (R Core Team, 2020), using the 'make.simmap' function in the package 'Phytools' (Revell, 2012). Reconstructions were performed under the 'equal rates' (ER) and the 'all rates different' (ARD) models, comparing the fit of the models with a likelihood ratio test using the function 'pchisq'. The ER model was selected for the characters 'organization of euryteles' and 'substrate choice', whereas the ARD model for the characters 'cnidocyst pouches' and 'host'. 10000 stochastic mapping replicates were conducted for each analysis and the results were summarized with pie charts representing the posterior probability of each internal node being in each state.

DNA-based species discovery and validation

Distance- and tree-based species delimitation approaches were used to investigate the presence of multiple species hypotheses in octocoral-associated *Pteroclava*. All analyses were run separately on

the single-locus datasets, keeping only *Pteroclava* sequences and collapsing the alignments into haplotypes by removing identical sequences, using FaBox (Villesen, 2007). Sequences with different length but identical nucleotides were considered the same haplotype.

The distance-based Automatic Barcode Gap Discovery (ABGD; Puillandre et al., 2012) and Assemble Species by Automatic Partitioning (ASAP; Puillandre et al., 2020) methods were performed using matrices of genetic distances (Kimura 2-Parameter) as inputs. The ABGD delimitations were run on the website 'abgd web' (https://www.abi.snv.jussieu.fr/public/abgd/abgdweb.html), setting parameters as follows: $P_{min} = 0.001$, $P_{max} = 0.1$, Steps = 100, X = 1.5, Nb bins = 100. The ASAP delimitations were run on the website 'asap web' (https://bioinfo.mnhn.fr/abi/public/asap/) considering only the partitions showing the lowest asap-score.

For tree-based methods, single-locus ML trees were obtained as described above and ultrametric Bayesian trees were obtained with BEAST 1.8.2 (Drummond et al., 2012), setting a coalescent tree prior and an uncorrelated lognormal relaxed clock. Three replicate analyses were run for 10^8 million generations, with trees sampled every 10000th generation, and were combined using LogCombiner 1.8.2 (Drummond et al., 2012) with a burn-in set to 25%. Maximum clade credibility trees were obtained using TreeAnnotator 1.8.2 (Drummond et al., 2012). The obtained trees were used as inputs for the Poisson Tree Process (PTP) and Generalized Mixed Yule Coalescence (GMYC) methods. Multiple-threshold PTP analyses (mtPTP: Kapli et al., 2017) were performed on the website 'mPTP Webservice' (https://mptp.h-its.org) using ML trees as input, whereas GMYC analyses were run in the R environment (R Core Team, 2020), using ultrametric trees as input. Specifically, single-threshold GMYC (stGMYC; Pons et al., 2006) and bGMYC (Reid and Carstens, 2012) analyses were run using the packages 'Splits' (Ezard et al., 2009), 'Ape' (Paradis et al., 2004), and 'bGMYC' (Reid and Carstens, 2012). bGMYC analyses were performed using a subset of 100 trees retrieved from the 10000 posterior trees obtained with each BI analysis. Single-threshold PTP and multiple-threshold GMYC methods were previously shown to be outperformed by the other implementations of PTP and GMYC used in this work (Fujisawa and Barraclough, 2013; Kapli et al., 2017) and were therefore not included in the analyses.

To validate the species hypotheses proposed by the single-locus analyses, the multi-locus dataset was analyzed under the multispecies coalescent model using Bayesian Phylogenetics and Phylogeography (BPP) 3.4 (Yang and Rannala, 2010). The algorithm A11 (joint species delimitation and species tree inference) was used and different values of the root age (τ) and prior distributions of the ancestral population size (θ) were tested, due to the lack of knowledge about these parameters in *Pteroclava* and to test their possible influence on the number of delimited species (Leaché and Fujita, 2010). We tested for: (i) large ancestral population size and deep divergence [$\theta \sim$ IG (3, 0.04), $\tau \sim$ IG (3, 0.02)]; (ii) small ancestral population size and shallow divergence [$\theta \sim$ IG (3, 0.004), $\tau \sim$ IG (3, 0.002)]; (iii) small ancestral population size and deep divergence [$\theta \sim$ IG (3, 0.004), $\tau \sim$ IG (3, 0.02)]; (iv) large ancestral population size and shallow divergence [$\theta \sim$ IG (3, 0.04), $\tau \sim$ IG (3, 0.002)]. Each analysis was run using both the reversible-jump MCMC algorithm 0 ($\varepsilon = 1$) and algorithm 1 ($\alpha = 1.5$, m = 1.5) to assess the impact of the fine-tuning parameters of reversible-jump algorithms on the speciation probabilities, and was repeated two times, to confirm the stability of results across runs. For each run, 50000 samples were collected with a sampling frequency of 10 iterations after a burn-in of the first 5000 cycles.

Finally, DNA diagnostic characters were searched for each *P. krempfi* clade, using the package QUIDDICH (Kühn and Haase, 2020) in the R environment (R Core Team, 2020). Specifically, character attributes (i.e., single nucleotides) present in all members of a defined clade but absent in members of other clades were searched, and the analyses were run for each molecular marker, considering different species hypotheses.

Alignments and raw phylogenetic trees are provided as supplementary files.

Pteroclava cnidocyst size analyses

To explore differences in the size of cnidocysts among *P. krempfi* clades, we selected 15 colonies, five for each of the clades Ia, IIa, and III, whereas measurements were not performed for clades Ib and IIb (Fig. 2), since insufficient material was available. The analyzed colonies were associated with nine different hosts and collected from five localities. For each colony, ten polyps were selected and, for each polyp, up to 15 capsules per type were measured. The descriptive statistical parameters of all cnidocyst types [length, width (mean ± sd), range (maximum-minimum)] were calculated for each clade in the R environment (R Core Team, 2020) using the 'Rcmdr' package (Fox and Bouchet-Valat, 2020). Kernel density plots (Sheather, 2004) were produced for the length of each cnidocyst type and clade. Stratified box plots for each cnidocyst type, clade, locality and host were also obtained. All graphics were made using the package 'ggplot2' (Wickham, 2016).

To study the variation of cnidocyst sizes in the *P. krempfi* clades, linear mixed models (LMM) or generalized linear mixed models (GLMM) were fitted for each of the three cnidocyst types (eurytele, large stenotele, small stenotele). Only the length data were used, since width data are in general less variable (Garese et al., 2016). The selection of LMM or GLMM was performed assessing the normality or not of the residuals of the models (following Garese et al., 2016). The models were performed using the R package 'lme4' (Bates et al., 2015). The general form of the models was: $y_i = \beta_i x + z_i \mu_i + \varepsilon_i$, where y is the response variable, β_i is the fixed effect parameter, μ_i is the random effect parameter, x is the matrix of fixed parameters, z is the matrix of random effects and ε_i is the matrix of errors. The global model form included 'cnidocyst size' as the dependent variable and 'clade' as fixed effect. Since datasets were assembled by measuring polyps from different colonies, localities, and/or hosts, these variables were at first considered as random effects and then their significance evaluated. By consequence, the global model form was: Cnidocyst sizes ~ Clade + (1|Polyp) + (1|Colony) + (1|Locality) + (1|Host) + ε.

To find the best model, the significance of each random effect was tested by deleting them one by one, using 'ranova' function of the R package 'lmerTest' (Kuznetsova et al., 2017), and to rank LMMs or GLMMs the Akaike Information Criterion (AIC) was used. Once the best model was determined, the normality of residuals of the LMM were tested by Shapiro–Wilks test and, graphically, in QQ-plots, and the homoscedasticity of variance was checked in fitted vs residual graphs. When the assumption of normality was not met, a GLMM was fitted by maximum likelihood (Laplace Approximation) with Gamma distribution for errors and inverse link function. Then, the best models were compared through ANOVA with a null model (Cnidocyst sizes ~ Clade) to test the significance of the LMM or GLMM. Finally, the model estimates for each clade, the confidence intervals, and the standard deviation for random effects, were extracted and analyzed. The R scripts used for the LMM and GLMM are shown in File S1.

Results

A total of 75 colonies were collected from the studied localities and identified as *Cladocoryne floccosa*, *C. haddoni*, *Pteroclava krempfi* and *Zanclea timida*.

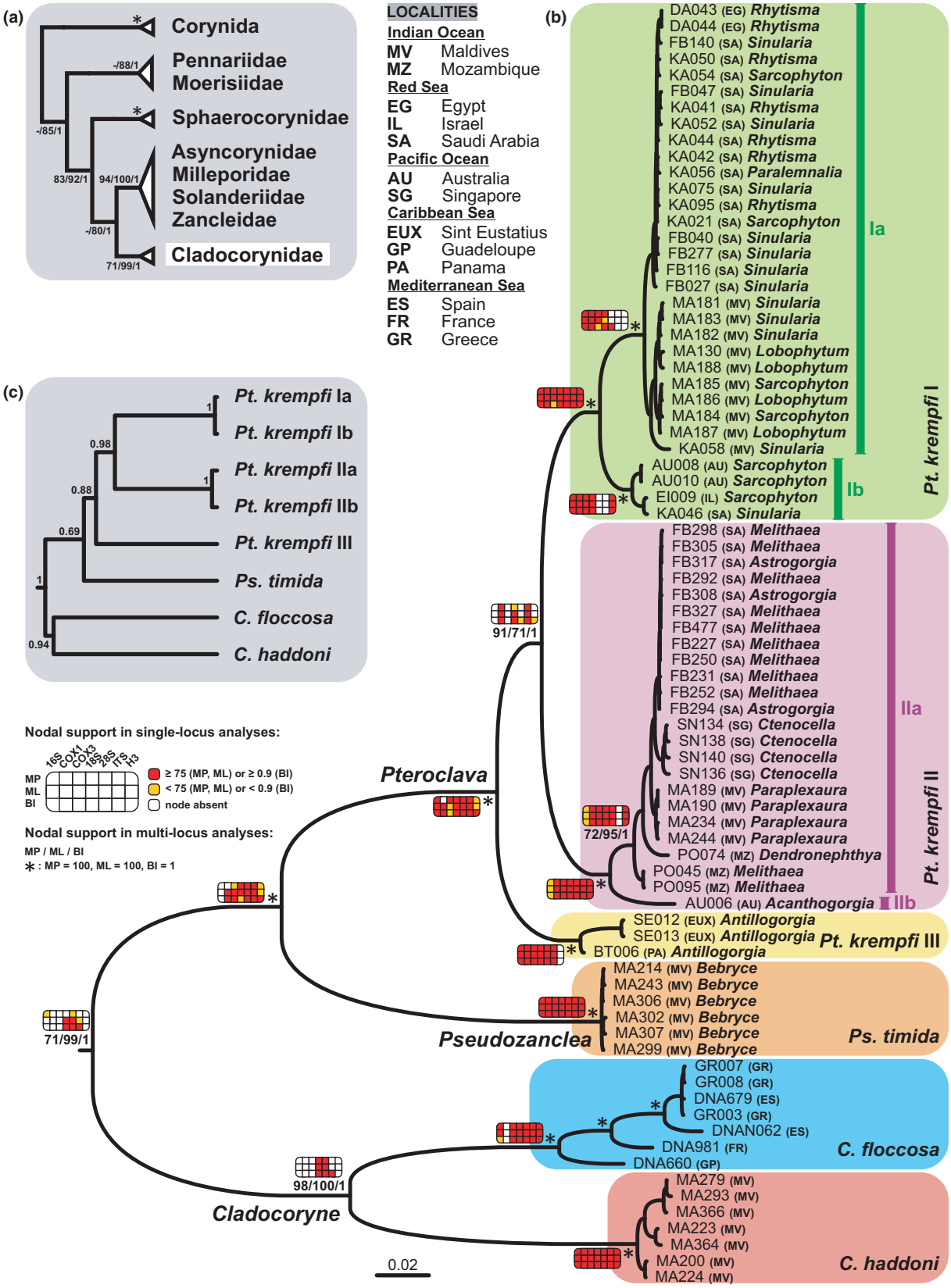
(a)
Corynida
Pennariidae
Moerisiidae
Sphaerocorynidae
Asyncorynidae
Milleporidae
Solanderiidae
Zancleidae
Cladocorynidae
*
-/88/1
*
-/85/1
83/92/1
94/100/1
-/80/1
71/99/1
LOCALITIES
Indian Ocean
MV Maldives
MZ Mozambique
Red Sea
EG Egypt
IL Israel
SA Saudi Arabia
Pacific Ocean
AU Australia
SG Singapore
Caribbean Sea
EUX Sint Eustatius
GP Guadeloupe
PA Panama
Mediterranean Sea
ES Spain
FR France
GR Greece
(b)
DA043 (EG) Rhytisma
DA044 (EG) Rhytisma
FB140 (SA) Sinularia
KA050 (SA) Rhytisma
KA054 (SA) Sarcophyton
FB047 (SA) Sinularia
KA041 (SA) Rhytisma
KA052 (SA) Sinularia
KA044 (SA) Rhytisma
KA042 (SA) Rhytisma
KA056 (SA) Paralemnalia
KA075 (SA) Sinularia
KA095 (SA) Rhytisma
KA021 (SA) Sarcophyton
FB040 (SA) Sinularia
FB277 (SA) Sinularia
FB116 (SA) Sinularia
FB027 (SA) Sinularia
MA181 (MV) Sinularia
MA183 (MV) Sinularia
MA182 (MV) Sinularia
MA130 (MV) Lobophytum
MA188 (MV) Lobophytum
MA185 (MV) Sarcophyton
MA186 (MV) Lobophytum
MA184 (MV) Sarcophyton
MA187 (MV) Lobophytum
KA058 (MV) Sinularia
AU008 (AU) Sarcophyton
AU010 (AU) Sarcophyton
EI009 (IL) Sarcophyton
KA046 (SA) Sinularia
Ia
Ib
Pt. krempfi I
FB298 (SA) Melithaea
FB305 (SA) Melithaea
FB317 (SA) Astrogorgia
FB292 (SA) Melithaea
FB308 (SA) Astrogorgia
FB327 (SA) Melithaea
FB477 (SA) Melithaea
FB227 (SA) Melithaea
FB250 (SA) Melithaea
FB231 (SA) Melithaea
FB252 (SA) Melithaea
FB294 (SA) Astrogorgia
SN134 (SG) Ctenocella
SN138 (SG) Ctenocella
SN140 (SG) Ctenocella
SN136 (SG) Ctenocella
MA189 (MV) Paraplexaura
MA190 (MV) Paraplexaura
MA234 (MV) Paraplexaura
MA244 (MV) Paraplexaura
PO074 (MZ) Dendronephthya
PO045 (MZ) Melithaea
PO095 (MZ) Melithaea
AU006 (AU) Acanthogorgia
IIa
IIb
Pt. krempfi II
SE012 (EUX) Antillogorgia
SE013 (EUX) Antillogorgia
BT006 (PA) Antillogorgia
Pt. krempfi III
MA214 (MV) Bebryce
MA243 (MV) Bebryce
MA306 (MV) Bebryce
MA302 (MV) Bebryce
MA307 (MV) Bebryce
MA299 (MV) Bebryce
Ps. timida
GR007 (GR)
GR008 (GR)
DNA679 (ES)
GR003 (GR)
DNAN062 (ES)
DNA981 (FR)
DNA660 (GP)
C. floccosa
MA279 (MV)
MA293 (MV)
MA366 (MV)
MA223 (MV)
MA364 (MV)
MA200 (MV)
MA224 (MV)
C. haddoni
(c)
Pt. krempfi Ia
Pt. krempfi Ib
Pt. krempfi IIa
Pt. krempfi IIb
Pt. krempfi III
Ps. timida
C. floccosa
C. haddoni
1
0.98
1
0.88
0.69
1
0.94
Nodal support in single-locus analyses:
16S
COX1
COX3
18S
28S
ITS
H3
MP
ML
BI
≥ 75 (MP, ML) or ≥ 0.9 (BI)
< 75 (MP, ML) or < 0.9 (BI)
node absent
Nodal support in multi-locus analyses:
MP / ML / BI
*: MP = 100, ML = 100, BI = 1
91/71/1
72/95/1
Pteroclava
71/99/1
Pseudozanclea
98/100/1
Cladocoryne
0.02

Fig. 2. Phylogenetic hypotheses of the Cladocorynidae. (a) Cladogram showing the phylogenetic placement of the Cladocorynidae in the superfamily Zancleida and (b) ML tree showing the phylogenetic relationships among the cladocorynid species, based on the concatenated multi-locus dataset. (c) Species tree of the cladocorynid species. Numbers at nodes in (a) and (b) represent bootstrap values of MP and ML analyses, and Bayesian posterior probabilities of BI analyses, respectively, for the multi-locus analyses, with asterisks indicating maximal nodal support for all analyses; nodal supports obtained with single-locus analyses are shown in panels, coloured as coded in the legend. In (c) numbers only represent Bayesian posterior probabilities. In (b) clades are highlighted with different colours and alphanumeric codes; sampling localities, as coded in the legend, and hosts are also reported for each terminal taxon.

The morphology of all investigated species corresponded to the original descriptions, with the exception of *Z. timida*, as reported in the 'Taxonomic account' section. Indeed, the morphological analysis of the medusa stage of *Z. timida*, conducted herein for the first time, highlighted strong similarities with the medusa of *P. krempfi,* specifically the presence of eurytheles in the exumbrellar cnidocyst pouches. On the other hand, the polyp stage was not ascribable to the genus *Pteroclava*, being more similar to typical *Zanclea* polyps (i.e., with oral and aboral capitate tentacles). For these reasons, and in accordance with phylogenetic results, the new cladocorynid genus *Pseudozanclea* gen. nov. was established to accommodate *Z. timida*, resulting in the new combination *Pseudozanclea timida* comb. nov.

In addition, specimens from Mozambique, Singapore, and Australia represent new geographic records for *P. krempfi*. The host range of the *Pteroclava*-octocoral association was also widened with the inclusion of the alcyonacean genera *Melithaea* Milne Edwards, 1857 (family Melithaeidae Gray, 1870), *Ctenocella* Valenciennes, 1855 (Ellisellidae Gray, 1859), *Acanthogorgia* Gray, 1857 (Acanthogorgiidae Gray, 1959), *Dendronephthya* Kükenthal, 1905 and *Paralemnalia* Kükenthal, 1913 (Nephtheidae Gray, 1862). Therefore, *P. krempfi* is currently known to live in association with 14 octocoral genera belonging to seven families (Table 2).

Molecular phylogenetics and species delimitation

The length of single-locus alignments was 625 bp for the 16S rRNA, 677 bp for COX1, 668 bp for COX3, 1712 bp for 18S rRNA, 1684 bp for 28S rRNA, 662 bp for ITS (927 bp before the Gblocks treatment), and 352 bp for H3 (Table 1), resulting in a total of 6380 bp for the concatenated alignment. Overall, the molecular markers were amplified and sequenced with high success (Table 3) and approximately 80% of the terminals in the concatenated dataset were represented by all markers. When this was not the case, one to three markers were missing (Table S1). The single- and multi-locus phylogeny reconstructions were broadly concordant (Fig. 2a, b; Fig. S1; Table S3). Although the relationships among clades varied across the single-locus analyses, each of the analyzed colonies belonged to the same molecular clade in almost all trees and phylogeny reconstruction criteria (Table S3). Multi-locus analyses resulted in the same ingroup topology with high nodal support (Fig. 2a, b), with only minor variation in the relationships among outgroups (Fig. 2a; Fig. S1). Here we considered the node support as maximal when bootstrap values (BS) for MP and ML analyses were = 100 and Bayesian posterior probabilities (BPP) = 1, high when BS $\geq$ 75 and BPP $\geq$ 0.9, and low when BS < 75 and BPP < 0.9. The family Cladocorynidae was monophyletic in all multi-locus analyses, with maximal support in ML and BI analyses, and lower support in the MP analysis (BS = 71), and its phylogenetic position as sister group of the families Asyncorynidae Kramp, 1949, Milleporidae Fleming, 1828, Solanderiidae Marshall, 1892, and Zancleidae Russel, 1953 was confirmed (Fig. 2a, Fig. S1). Both cladocorynid genera, *Cladocoryne* and *Pteroclava*, and all the analyzed species, were consistently recovered as monophyletic with high or maximal support values (Fig. 2b). All the specimens belonging to *Pseudozanclea timida*, and collected in the Maldives, formed a monophyletic clade that was sister to *Pteroclava* in all multi-locus analyses with maximal nodal support. The phylogenetic placement of this species within the Cladocorynidae was therefore demonstrated, supporting the transfer from the genus *Zanclea* and family Zancleidae to the new genus *Pseudozanclea*. In all analyses, *Pteroclava krempfi* was characterized by a strong intra-specific genetic variation, spanning in most cases five well-supported clades (Fig. 2b; Fig. S1; Table S3): *Pteroclava krempfi* Ia, Ib, IIa, IIb, and III. The clades *P. krempfi* I, II, and III were recovered in all analyses, whereas sub-clades Ia, Ib, IIa, and IIb were recovered in most analyses, with the exception of single-locus ITS, 28S, and H3 analyses (Table S3).

The genetic distances among the nominal species were high for all DNA regions, with nuclear 18S and 28S rRNA showing the lowest values, whereas intra-specific distances were low for all species but *P. krempfi* and *C. floccosa* (Table 4; Table S4). These two species showed high intra-specific distances especially in mitochondrial regions, with values of 4.7% for *P. krempfi* and 3.7% for *C. floccosa* for the 16S rRNA dataset (Table S4). Regarding *P. krempfi*, the inter-clade genetic distances were also generally high,

Table 2
Host range of *Pteroclava krempfi*

Host	Distribution	Clade
fam. Alcyoniidae		
Cladiella	Vietnam*	unknown*
Lobophytum	Maldives	Ia
Rhytisma	Red Sea (Egypt, Saudi Arabia)	Ia
Sinularia	Maldives, Red Sea (Saudi Arabia)	Ia, Ib
Sarcophyton	Australia, Maldives, Red Sea (Israel, Saudi Arabia)	Ia, Ib
fam. Acanthogorgiidae		
Acanthogorgia	Australia	IIb
fam. Ellisellidae		
Ctenocella	Singapore	IIa
fam. Gorgoniidae		
Antillogorgia	Caribbean (Panama, Sint Eustatius)	III
fam. Melithaeidae		
Melithaea	Mozambique, Red Sea (Saudi Arabia)	IIa
fam. Nephtheidae		
Dendronephthya	Mozambique	IIa
Paralemnalia	Red Sea (Saudi Arabia)	Ia
fam. Plexauridae		
Astrogorgia	Red Sea (Saudi Arabia), Indonesia*	IIa, unknown*
Paraplexaura	Maldives	IIa
Plexaurella	Caribbean (Cuba)*	unknown*

*Data from literature.

Table 3
Summary of sequencing results for each species/clade, showing the % of successfully sequenced specimens for each DNA region

Species/Clade (No. of specimens)	16S	COX1	COX3	18S	28S	ITS	H3	Conc
Cladocoryne floccosa (n = 7)	100	0	100	100	100	43	86	0
Cladocoryne haddoni (n = 7)	100	100	100	100	100	100	86	86
Pseudozanclea timida (n = 6)	100	100	100	100	100	100	100	100
Pteroclava krempfi Ia (n = 28)	100	100	100	100	100	100	100	100
Pteroclava krempfi Ib (n = 4)	100	100	100	100	100	100	100	100
Pteroclava krempfi IIa (n = 23)	100	100	100	100	100	100	100	100
Pteroclava krempfi IIb (n = 1)	100	0	100	0	100	100	100	0
Pteroclava krempfi III (n = 3)	100	67	67	100	100	100	33	0
Outgroups (n = 12)	100	83	92	100	100	92	75	58
Total (n = 91)	100	88	95	99	100	95	92	78

The column 'Conc' refers to the % of terminals with all markers sequenced in the concatenated dataset

and a reasonable decrease in the intra-clade distances was observed by grouping sequences in the five clades obtained with phylogenetic analyses, with no overlap with intra-clade distances (Table 4; Table S4).

Single-locus DNA-based species delimitation analyses of *P. krempfi* showed variable results, according to the method used and DNA region analyzed (Fig. 3a), and resulted in five possible scenarios, spanning one to five species hypotheses (Fig. 3b). According to phylogenetic and genetic distance analyses, the delimitation based on mitochondrial regions revealed the highest number of species hypotheses, whereas those based on nuclear regions mostly retrieved three species hypotheses (Fig. 3a). The BPP multi-locus delimitation analyses consistently inferred a five-species model with high posterior support (always > 0.99), regardless of the algorithm and sets of priors used. Consistently, the posterior probabilities for each of the five delimited species hypotheses were always high (> 0.99) (Table S5).

Diagnostic characters were searched in *P. krempfi* clades considering the three-species model and the five-species model (Table S6). In the three-species model, diagnostic characters were detected for all clades and molecular markers, with highest numbers in the mitochondrial COX1 and COX3 genes and the ITS. On the other hand, in the five-species model diagnostic characters were found for all clades only in the 16S rRNA and COX3 genes. Overall, clade III consistently showed the highest number of diagnostic characters in all DNA regions.

A species tree of the Cladocorynidae family was produced considering *P. krempfi* as composed of five

Table 4
16S rRNA genetic distances shown as % uncorrected *p*-distance (± standard deviation) among and within *Pteroclava krempfi* clades

Pt. krempfi Ia	1.0 (±0.2)				
Pt. krempfi Ib	4.4 (±0.7)	1.0 (±0.3)			
Pt. krempfi IIa	6.9 (±0.9)	6.8 (±0.9)	1.1 (±0.2)		
Pt. krempfi IIb	7.5 (±1.0)	7.2 (±1.0)	4.3 (±0.7)	n.c.	
Pt. krempfi III	8.8 (±1.3)	9.3 (±1.3)	9.3 (±1.3)	9.0 (±1.3)	1.8 (±0.5)

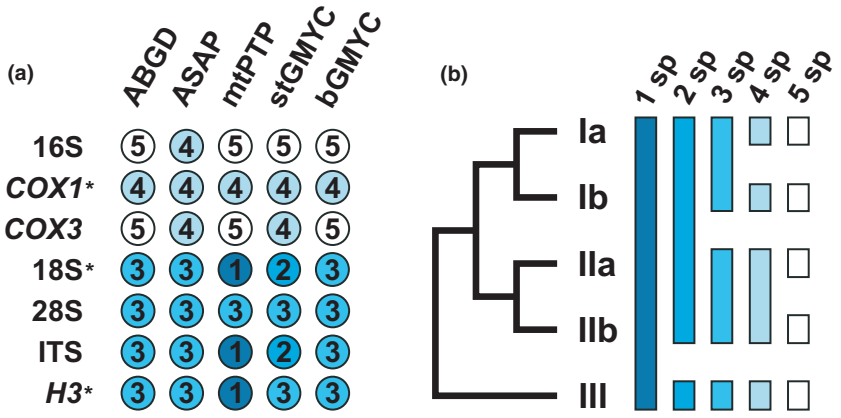

Fig. 3. Single-locus species delimitation summary of *Pteroclava krempfi*. (a) Number of species hypotheses obtained analysing different DNA regions and using different methods. (b) Five possible scenarios, ranging from one to five species within *P. krempfi*, as obtained with species delimitation analyses. *Clade IIb not sequenced.

species (Fig. 2c). The topology of the species tree was identical to that of the concatenated multi-locus trees, although an overall lower support was obtained (Fig. 2b, c). Specifically, the relationships among *Pteroclava* clades did not vary, *Pseudozanclea timida* was confirmed as the sister group of *Pteroclava*, and *Cladocoryne* as the sister group of *Pteroclava* + *Pseudozanclea*.

According to the ancestral state reconstructions, the organisation of euryteles in clusters or rings in the polyp stage (Fig. 4a) and the presence of exumbrellar cnidocyst pouches with euryteles in the medusa (Fig. 4b) resulted to likely be synapomorphies of the Cladocorynidae, being appeared in the most recent common ancestor (MRCA) of the extant family members. The establishment of symbiotic relationships between the polyp stage and other benthic organisms used as substrates emerged multiple times in the superfamily Zancleida (Fig. 4c), but the association with octocorals probably emerged in the MRCA of the *Pteroclava* + *Pseudozanclea* clade (Fig. 4d).

Distribution, host specificity, and geographic structure of Pteroclava clades

Both *Pteroclava krempfi* clades I and II were found across the Indo-Pacific and Red Sea, whereas clade III was exclusively observed in Caribbean localities and associated with *Antillogorgia*. Clade I was associated with members of the octocoral family Alcyoniidae (*Sinularia*, *Sarcophyton*, *Lobophytum*, *Rhytisma*), with the only exception of a colony associated with *Paralemnalia* (family Nephtheidae) (Table 2). Clade Ib included four colonies collected in the Red Sea and Australia, associated with *Sarcophyton* and *Sinularia* octocorals, whereas the remaining specimens belonged to clade Ia. Within clade I, no clear host-related genetic structure was observed (Fig 4a), with two haplotypes associated with multiple hosts, whereas populations from the Indian Ocean and Red Sea appeared to be moderately differentiated, with the exception of a Red Sea haplotype more related to Indian Ocean haplotypes (Fig. 5b). Clade II was composed of clade IIa, associated with the genera *Astrogorgia* and *Paraplexaura* (Plexauridae), *Melithaea* (Melithaeidae), *Ctenocella* (Ellisellidae) and *Dendronephthya* (Nephtheidae), and clade IIb, represented by a single colony associated with *Acanthogorgia* (Acanthogorgiidae) (Table 2). In clade II no host-related genetic structure was also clearly detectable, and the most common haplotype was associated with two different octocoral genera (Fig. 5c). Clade II showed a lower number of haplotypes compared to clade I and in this case different localities did not share the same haplotypes, even if a clear geographic pattern was not observed (Fig. 5d).

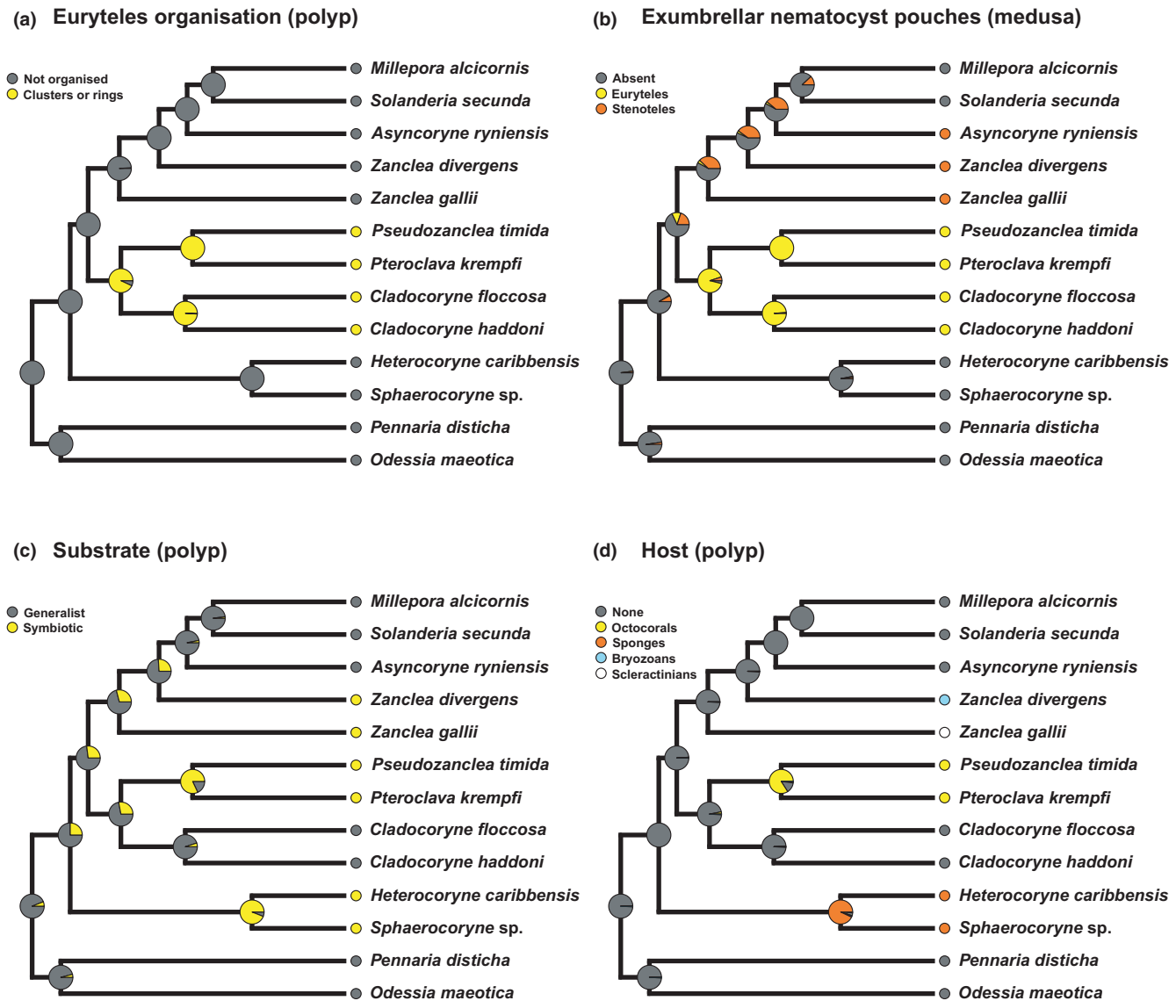

Fig. 4. Stochastic character maps showing the ancestral state reconstruction of the characters (a) eurytele organization in polyps, (b) exumbrellar nematocyst pouches in medusae, (c) substrate on which polyp colonies grow, (d) host of polyp colonies. Pie charts represents the posterior probability of each node being in each state.

Morphometry of the Pteroclava polyp cnidome

The cnidome of *P. krempfi* polyps was composed of stenoteles of two size classes (small and large) located in the tentacles and macrobasic apotrichous euryteles below the hypostome. A total of 5816 capsules were measured (Table S7), and the raw data reflected similarities in cnidocyst size among the three investigated clades (Ia, IIa, and III), as shown in Table S8. The eurytele length of clade III was slightly larger than Ia and IIa, even if the ranges of the three clades were partially overlapping. Furthermore, eurytele width was slightly larger in clade III. All other measurements were not noticeably different among the investigated clades.

The distributions of cnidocyst length for each cnidocyst type and clade are reported in the density plots in Fig. 5a–c, showing the general overlapping of the length distributions and the higher values for eurytele length in clade III (Fig. 6a). Fig. 5d–f show the stratified box plots of the length measurements for each cnidocyst type, clade, host, and locality investigated. The larger size of euryteles of clade III can be observed in Fig. 6d, whereas clade Ia from the Red Sea showed the smallest size. The size of both large and small stenoteles appeared to be very similar

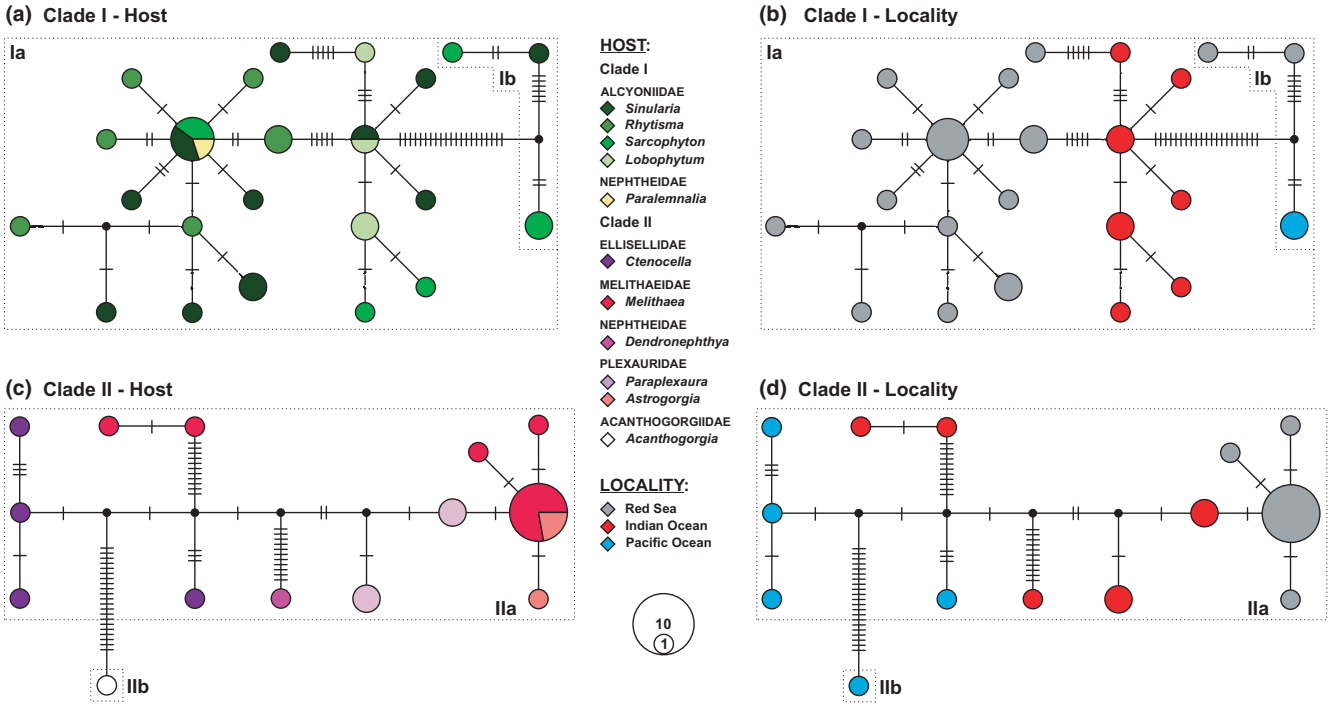

Fig. 5. 16S rRNA most parsimonious median-joining haplotype networks of *Pteroclava krempfi* (a, b) clade I and (c, d) clade II. Haplotypes are coloured by (a, c) host and (b, d) sampling locality for both clades, as shown in the legend, and sub-clades are delimited by dashed lines. Each cross-bar represents a single nucleotide change, and small black circles represent missing haplotypes.

among the three clades from different hosts and localities (Fig. 5e, f), with the largest values observed in specimens belonging to clade IIa associated with *Melithaea* in the Red Sea.

The best model produced by model selection was: Cnidocyst sizes ~ Clade + (1|Polyp) + (1|Colony) + ε. For all cnidocyst types, both 'Polyp' and 'Colony' were significant, whereas 'Locality' and 'Host' were not (Table S9). For eurytheles and large stenoteles, a LMM was fitted according to the normality of the residuals ($P = 0.4805$ and $P = 0.2207$, respectively; $\alpha = 0.05$) (Fig. S2) from the best models. For small stenoteles, the residuals of the best LMM did not fit the normal distribution ($P = 0.001$; $\alpha = 0.05$), therefore a GLMM was fitted. The best models for eurytele and stenotele large (LMMs), and stenotele small (GLMM) were significant versus the null models (Table 5). Estimates and confidence intervals (CIs) of the models for each clade are shown in Table 6, and the standard deviation of the random effects 'Polyp' and 'Colony' for each cnidocyst type are shown in Table S10.

Eurytheles of the clade III showed an estimated value for cnidocyst length larger than Ia and IIa. Moreover, the CIs for clade III did not overlap with the CIs of clade Ia, and only partially overlapped with the CIs of clade IIb. On the other hand, estimates for clade Ia and Ib were very similar, with almost totally overlapping CIs (Table 6). Although both 'Polyp' and 'Colony' as random effects were significant, their standard deviations were small, around 1 μm and 2 μm, respectively (Table S10), suggesting no considerable variation within polyps and colonies. The model estimates for both small and large stenoteles were almost identical for the three clades, with completely overlapping CIs and very small standard deviations of 'Polyp' and 'Colony' (Table 6; Table S10). Thus, no differences were detected in the length of stenoteles among clades.

Taxonomic account

Acronyms for the museums hosting cladocorynid material are as follows: Museo Civico di Storia Naturale, Cnidaria Collection, Milano (MSNMCOE), Natural History Museum, London (NHMUK), Muséum National d'Histoire Naturelle, Paris (MNHN), Australian Museum (AU), Museo di Storia Naturale Giacomo Doria, Genova (MSNG).

Hydrozoa Owen, 1843

Capitata Kühn, 1913

Cladocorynidae Allman, 1872

Amended diagnosis: Stem simple or slightly branched, arising from a creeping hydrorhiza. Oral tentacles capitate or moniliform, aboral tentacles

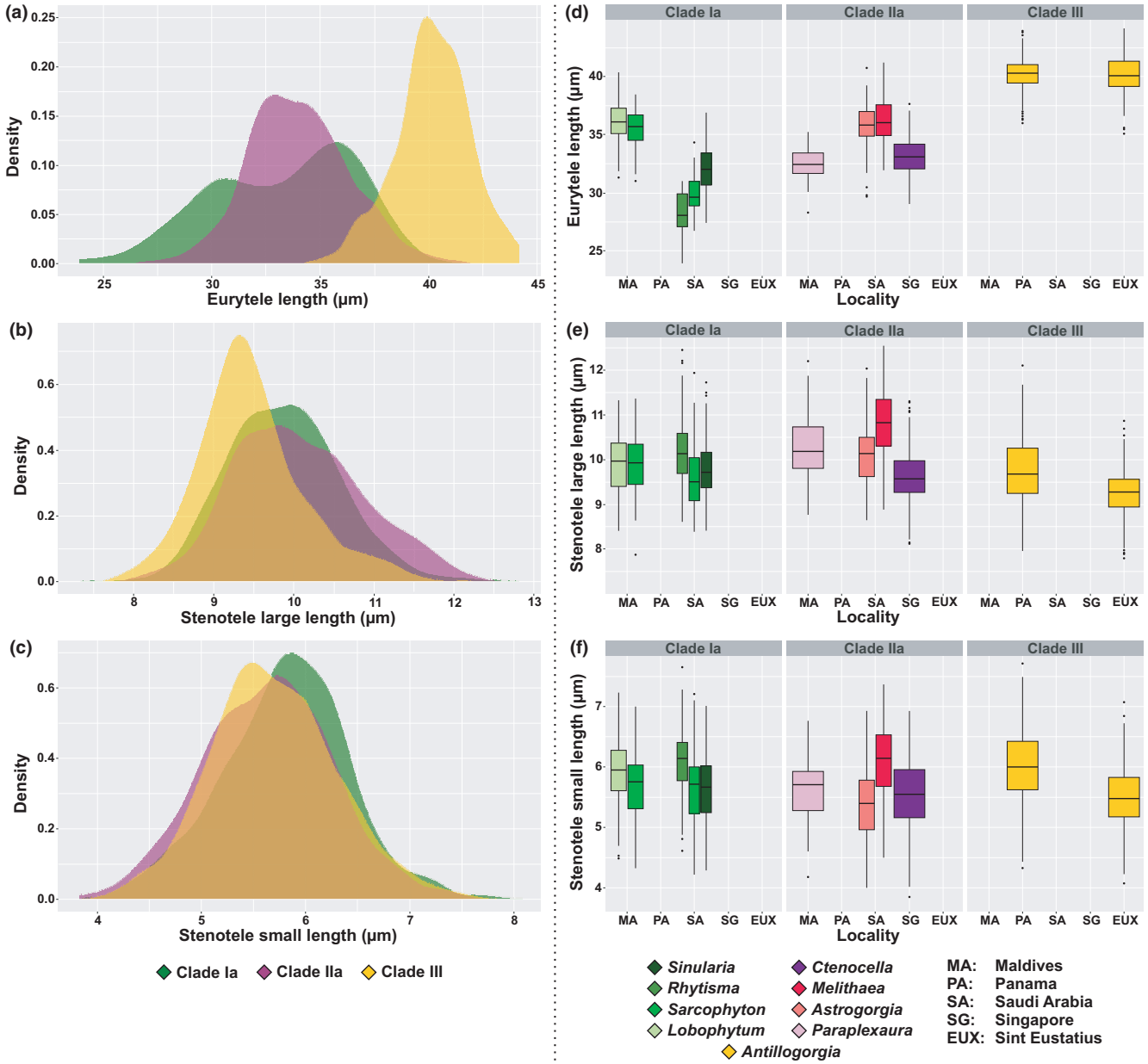

Fig. 6. Kernel density plots of the (a) eurytele, (b) large stenotele, and (c) small stenotele length for each *Pteroclava krempfi* clade (Ia, IIa, III). Stratified box plots for the length of (d) eurytele, (e) large stenotele, and (f) small stenotele, for each *P. krempfi* investigated clade, locality, and host.

moniliform, capitate, or branched capitate. Eurytele organized in patches or in a ring. Fixed cryptomedusoids or free-living medusae with exumbrellar pouches containing eurytele.

Cladocoryne Rotch, 1871

Type species: *Cladocoryne floccosa* Rotch, 1871

Diagnosis: Stem long arising from a creeping hydrorhiza covered by a perisarc. Polyps with oral whorl of short capitate tentacles, and one to four aboral whorls of branched-capitate tentacles. Eurytele organized in patches on hydranth body. Fixed cryptomedusoids.

Cladocoryne floccosa Rotch, 1871

See Schuchert (2006) for a complete synonymy.

Type locality: Herm, Channel Islands, United Kingdom

Type material: Holotype could not be located.

Newly deposited material: Colony collected in Corfu, Greece, 2 August 2018, fixed in formalin 10% (MSNMCOE348) and ethanol 99% (MSNMCOE349), DNA name GR003.

Description: Colonies growing on rock (Fig. 7a). Unbranched stems, sparingly annulated at some points

Table 5
ANOVA for the best models versus null models for each *Pteroclava krempfi* cnidocyst type

Model	npar	AIC	logLik	deviance	Chisq	Df	Pr(>Chisq)
Eurytele length–Species♦	4	6232.1	−3112.1	6224.1			
Eurytele length–Species + (1|Polyp) + (1|Colony)▲	6	4916.9	−2452.4	4904.9	1319.2	2	<2.2E-016***
Stenotele large length–Species♦	4	4919.7	−2455.9	4911.7			
Stenotele large length–Species + (1|Polyp) + (1|Colony)▲	6	4206.6	−2097.3	4194.6	717.16	2	<2.2E-016***
Stenotele small length–Species◇	4	3995.7	−1993.9	3987.7			
Stenotele small length–Species + (1|Polyp) + (1|Colony)►	6	3258.7	−1623.3	3246.7	741.04	2	<2.2E-016***

AIC, Akaike Information Criterion for the model evaluated as - *(logLik -npar); logLik, log-likelihood for the model; npar, number of parameters; ♦ null LMM; ▲ best LMM; ◇ null GLMM; ▶ best GLMM.
***Significance level: 0.001.

Table 6
Pteroclava krempfi cnidocyst length (μm) estimates and confidence intervals (CIs) from the models for each cnidocyst type and clade

Cnidocyst type/Clade	Estimate	Lower-95	Upper-95
Eurytele (n = 1335)			
Ia	32.45985	30.510483	34.409216
IIa	34.107214	29.399497	38.814931
III	40.025497	35.307838	44.743154
Stenotele large (n = 2248)			
Ia	9.8692909	9.5357731	10.20280875
IIa	10.069944	9.2647662	10.87512181
III	9.4704293	8.6652515	10.27560714
Stenotele small (n = 2233)			
Ia	5.7324277	5.4382122	6.0602992
IIa	5.5764185	4.9518472	6.3812832
III	5.6185172	4.983667	6.4387212

(Fig. 7b), up to 0.5 cm long and 140–200 μm wide, arising from creeping hydrorhiza. Perisarc stopping at the base of polyp. Polyps (Fig. 6c, d) up to 1.5 mm long with an oral whorl of 4–5 adnate capitate tentacles, up to 250 μm long, and three whorls of 4–6 ramified tentacles, up to 1.1 mm long, with up to 21 capitula disposed spirally and usually with three terminal capitula (Fig. 6e, f). Oral capitula larger than aboral capitula (~90 μm and ~55 μm wide, respectively), both with stenoteles of two size classes, with large stenoteles rare in aboral capitula. Up to five patches of macrobasic apotrichous euryteles among oral tentacles, up to three among aboral tentacles in the median whorl (not always present), and up to four among aboral tentacles in the proximal whorl. Polyps bearing up to four immature cryptomedusoids among the distal and median whorls of aboral tentacles (Fig. 7c), up to 0.35 mm long and 0.29 mm wide. Young cryptomedusoids without canals and bulbs, but with two exumbrellar pouches with euryteles (Fig. 7g). Living polyps transparent, sometimes with a reddish gastroderm and a white hypostome (Fig. 7a), living cryptomedusoids transparent with reddish manubrium.

Cnidome: Small stenoteles in capitula (5–7 × 4–6 μm) (Fig. 7h). Large stenoteles common in oral capitula and rare in aboral capitula (13–17 × 11–14 μm) (Fig. 7i). Macrobasic apotrichous euryteles in patches among oral and aboral tentacles and in pouches on the exumbrella (28–35 × 13–19 μm; discharged shaft: 190–200 μm) (Fig. 7j). All cnidocyst types found also in the stem and hydrorhiza and rarely in the hydranth.

Cladocoryne haddoni Kirkpatrick, 1890

See Schuchert (2003) for a complete synonymy.

Type locality: Murray Island, Torres Strait, Australia

Type material: Holotype – 1890.11.22.15-20 (NHMUK).

Newly deposited material: Colony collected in Central Maldives, 10 October 2015, fixed in formalin 10% (MSNMCOE346) and ethanol 99% (MSNMCOE347), DNA name MA200.

Description: Colonies growing on a variety of substrates, including rock, coralline algae, ascidians, and sponges (Fig. 8a). Unbranched stems up to 1 cm long and 185–195 μm wide, arising from creeping hydrorhiza. Perisarc stopping at the base of polyp. Polyps (Fig. 7b, c) up to 1.8 mm long with an oral whorl of 6–7 adnate capitate tentacles, up to 350 μm long, and two whorls of 5–8 ramified tentacles up to 1.2 mm long (Fig. 8d), with up to 30 capitula disposed spirally and usually with three terminal capitula (Fig. 8e). Oral capitula larger than aboral capitula (~90 μm and ~50 μm wide, respectively), both with stenoteles of two size classes, with large stenoteles rare in aboral capitula. Up to five patches of large macrobasic apotrichous euryteles in the area between oral and aboral tentacles (Fig. 8c). Smaller macrobasic apotrichous euryteles at the base or along some of the aboral tentacles. Polyps bearing up to two cryptomedusoids (only males observed), below eurytele patches and above aboral tentacles, up to 0.9 mm long and 0.6 mm wide (Fig. 8f). Cryptomedusoids with four rudimentary perradial canals ending in reduced tentacular bulbs with no tentacles, a rudimentary circular canal and pouches with large euryteles between bulbs (Fig. 8g). Manubrium large, bearing a white mass of

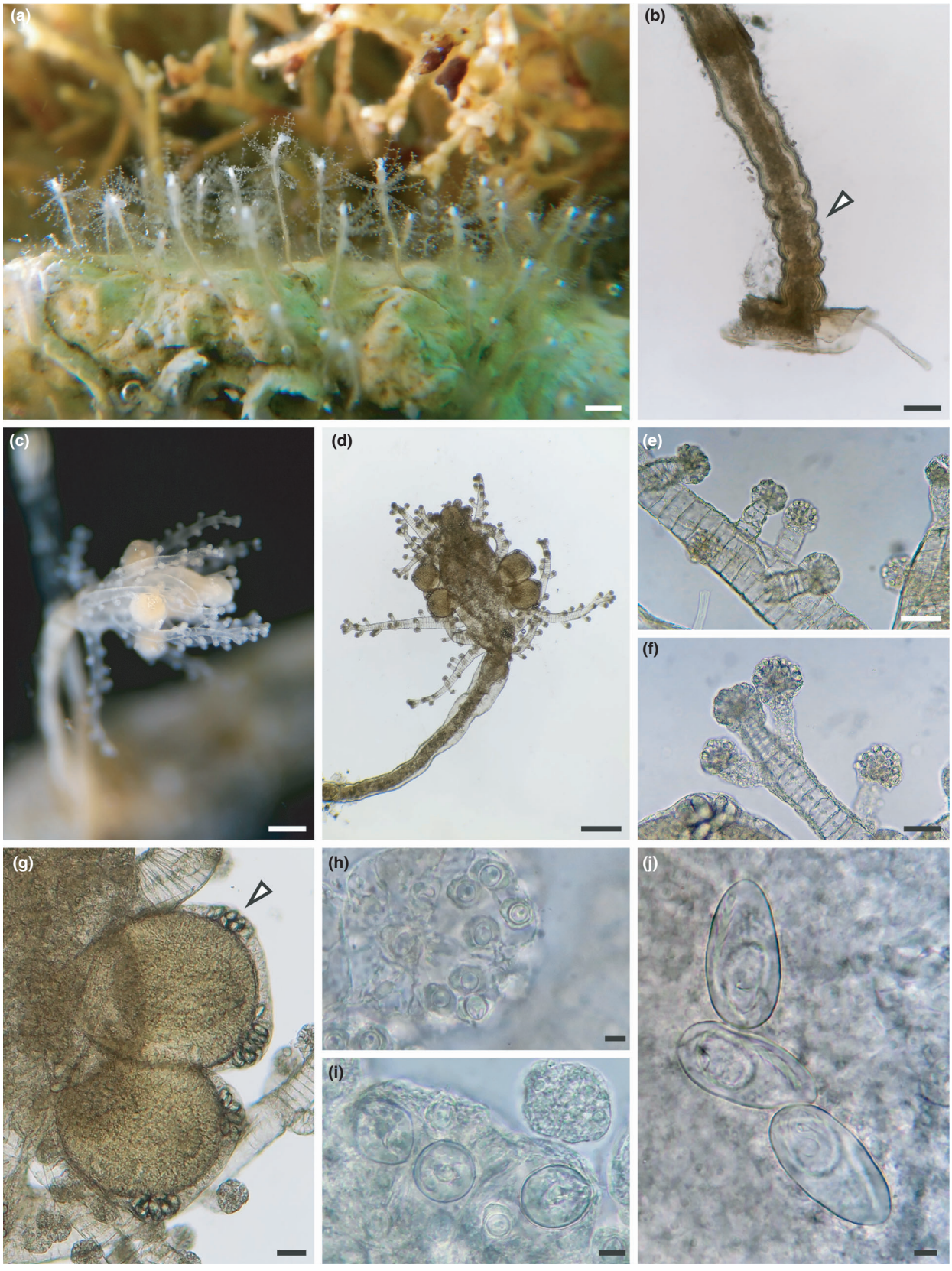
(a)
(b)
(c)
(d)
(e)
(f)
(g)
(h)
(i)
(j)

Fig. 7. *Cladocoryne floccosa*. (a) Living colony. (b) Proximal portion of the stem showing annulations (arrowhead). (c) Polyp (formalin-fixed) with four immature cryptomedusoids. (d) Same polyp under a compound microscope. (e) Aboral branching tentacle with ramifications arranged spirally. (f) Terminal ramifications of an aboral tentacle. (g) Close-up of two immature cryptomedusoids showing clusters of euryteles (arrowhead). (h) Small stenoteles. (i) Large stenoteles. (j) Macrobasic apotrichous euryteles. Scale bars: (a) 1 mm; (b) 150 μm; (c, d) 350 μm; (e–g) 50 μm; (h–j) 5 μm.

sperm. Stenoteles of two size classes and small euryteles sparingly scattered on the exumbrella. Living polyps transparent, with a reddish gastroderm and a white hypostome (Fig. 8a, b, f), cryptomedusoids transparent with reddish manubrium (Fig. 8f).

Cnidome: Small stenoteles in capitula and exumbrella (5–6 × 3–5 μm) (Fig. 8h). Large stenoteles common in oral capitula and rare in aboral capitula, and on exumbrella (10–14 × 9–11 μm) (Fig. 8i). Large macrobasic apotrichous euryteles in patches below oral tentacles and in pouches on the exumbrella (61–72 × 22–27 μm; discharged shaft: ~1.4 mm) (Fig. 8j). Small macrobasic apotrichous euryteles in tentacles and exumbrella (24–29 × 16–20 μm; discharged shaft: ~150 μm) (Fig. 8k). All cnidocyst types found also in the stem and hydrorhiza and rarely in the hydranth.

Pteroclava Weill, 1931

Type species: *Pteroclava krempfi* (Billard, 1919)

Diagnosis: Colonies growing on octocorals, with perisarc-covered hydrorhiza embedded in host tissues. Polyps with oral and aboral moniliform tentacles. Euryteles organized in patches on hydranth body. Medusae with pouches containing euryteles above atentaculate bulbs.

Pteroclava krempfi (Billard, 1919)

See Boero et al., (1995) and Puce et al., (2008) for a complete synonymy.

Type locality: Nha-Trang Bay, Vietnam.

Type material: Holotype – Type H.L. 020 (MNHN).

Newly deposited material: Colony collected in Central Red Sea, associated with *Sinularia* sp., 1 May 2017, fixed in formalin 10% (MSNMCOE350) and ethanol 99% (MSNMCOE351), DNA name FB047 (clade Ia); Colony collected in the Great Barrier Reef, Australia, associated with *Sarcophyton* sp., 13 November 2018, fixed in ethanol 99% (G18585; AM), DNA name AU008 (clade Ib); Colony collected in Central Maldives, associated with *Paraplexaura* sp., 13 April 2016, fixed in formalin 10% (MSNMCOE352) and ethanol 99% (MSNMCOE353), DNA name MA234 (clade IIa); Colony collected in the Great Barrier Reef, Australia, associated with *Acanthogorgia* sp., 14 November 2018, fixed in ethanol 99% (G18678; AM), DNA name AU006 (clade IIb); Colony collected in Caribbean Panama, associated with *Antillogorgia americana*, 18 August 2015, fixed in formalin 10% (MSNMCOE354) and ethanol 99% (MSNMCOE355), DNA name BT006 (clade III).

Description: Colonies living as partial endosymbionts of a variety of octocorals (Table 2, Fig. S3). Unbranched stems (up to 1.5 mm long) arising from creeping hydrorhiza embedded in host tissues (Fig. 9a). Perisarc stopping at the base of polyps (Fig. 9b). Polyps claviform up to 2 mm high, with 4–5 oral (up to 0.5 mm long) and 6–24 aboral (up to 1 mm long) moniliform tentacles scattered on the hydranth (Fig. 8a, b) with stenoteles of two size classes. Up to four rounded patches of macrobasic apotrichous euryteles below the oral tentacles, sometimes absent. Up to five medusa buds at the base or half of the polyp body, polyps often showing reproductive exhaustion (Fig. 9c). Newly liberated medusa (Fig. 9d) with a bell-shaped umbrella (up to 800 μm high and 850 μm wide), manubrium extending for 1/3 or 1/2 of the umbrella, and microbasic euryteles scattered on the exumbrella. Four perradial canals ending in two tentaculate bulbs and two smaller atentaculate bulbs. Atentaculate bulbs with an exumbrellar cnidocyst pouch containing up to four euryteles (Fig. 9e), the latter often found also in tentaculate bulbs. Tentacular bulbs bearing one tentacle each (Fig. 9f), about 1 mm long, with up to 40 ciliated rounded cnidophores approximately 25 μm wide, armed with 4–5 bean-shaped macrobasic apotrichous euryteles. Living polyps transparent, with a whitish hypostome and sometimes a reddish gastroderm (Fig. 9a), medusae transparent, with whitish or reddish manubrium.

Cnidome: Small stenoteles (4–8 × 3–7 μm) and large stenoteles (8–13 × 7–11 μm) in capitula (Fig. 8g, h). Macrobasic apotrichous euryteles in patches below oral tentacles, in exumbrellar pouches, and tentaculate bulbs (24–44 × 11–21 μm; discharged shaft: ~500) (Fig. 8e, i). Bean-shaped macrobasic apotrichous euryteles in cnidophores (6–10 × 4–6 μm; discharged shaft: 91–98 μm) (Fig. 9j). Microbasic euryteles on exumbrella (6–9 × 5–6 μm; discharged shaft: 15–16 μm) (Fig. 9k).

Pseudozanclea gen. nov. Maggioni & Montano

http://zoobank.org/ urn:lsid:zoobank.org:act:12328071-CED1-4765-9745-D114F3F8D33E

Type species: *Pseudozanclea timida* (Puce, Di Camillo and Bavestrello, 2008)

Diagnosis: Colonies growing on octocorals, with perisarc-free hydrorhiza embedded in host tissues. Polyps with oral and aboral capitate tentacles. Euryteles organized in a ring on hydranth body. Medusa

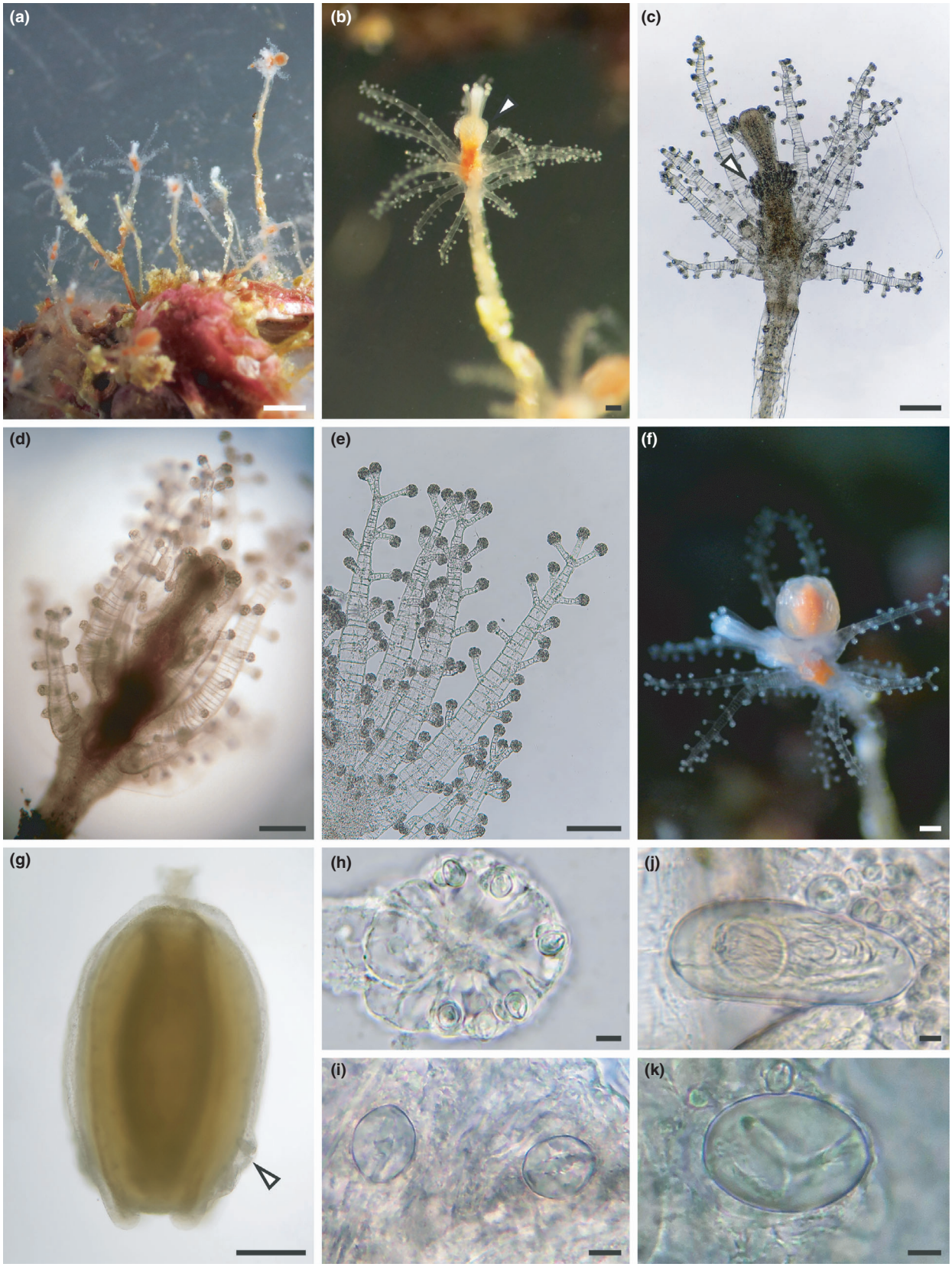
(a)
(b)
(c)
(d)
(e)
(f)
(g)
(h)
(j)
(i)
(k)

Fig. 8. *Cladocoryne haddoni*. (a) Living colony. (b, c) Polyps showing large euryteles patches below oral tentacles (arrowhead). (d) Polyp showing the two whorls of aboral tentacles. (e) Branching aboral tentacles showing ramifications spirally arranged with three terminal branches. (f) Polyp with a mature male cryptomedusoid. (g) Mature male cryptomedusoid detached from parental colony, with euryteles clusters on exumbrella (arrowhead). (h) Small stenoteles. (i) Large stenoteles. (j) Large macrobasic apotrichous eurytele. (k) Small macrobasic apotrichous eurytele. Scale bars: (a) 1.5 mm; (b–g) 200 μm; (h–k) 5 μm.

buds in tissue pockets until release. Medusae with pouches containing euryteles above atentaculate bulbs.

Etymology: The generic name refers to the similarity of the polyp stage to *Zanclea* polyps, and to the fact that the type species was previously ascribed to *Zanclea* genus.

Remarks: The establishment of the new genus is supported by both morphological and genetic data. Indeed, the polyp stage of *Pseudozanclea* differs from *Pteroclava* and *Cladocoryne* by showing a *Zanclea*-like morphology (i.e., hydranths with oral and aboral capitate tentacles) and the presence of peculiar tissue pockets containing medusa buds. Similarities with *Pteroclava* are observed in the newly released medusa, with exumbrellar pouches containing euryteles, and in the association with octocorals. These latter similarities are also reflected in the proposed phylogeny of the Cladocorynidae, with a sister group relationship between *Pteroclava* and *Pseudozanclea*.

Pseudozanclea timida comb. nov. (Puce, Di Camillo and Bavestrello, 2008)

Synonymy: *Zanclea timida* Puce et al., 2008: 1649, figs. 5c-e, 7; Maggioni et al., 2020a: 1, figs. 1d-f

Type locality: Siladen, North Sulawesi, Indonesia

Type material: Holotype – MSNG54191.

Newly deposited material: Colony collected in Central Maldives, associated with *Bebryce* cf. *grandicalyx*, 4 April 2016, fixed in formalin 10% (MSNMCOE344) and ethanol 99% (MSNMCOE345), and medusae released from the same colony fixed in formalin 10% (MSNMCOE343), DNA name MA243.

Description: Maldivian colonies associated with the octocoral *Bebryce* cf. *grandicalyx* and with a sponge in the family Suberitidae (Fig. 10a). Indonesian colonies associated with the octocoral *Paratelesto* sp. Perisarc-free hydrorhiza with clusters of macrobasic apotrichous euryteles (Fig. 10b), extending on the octocoral surface and completely covered by the sponge, when present. Polyps piriform, up to 0.9 mm long, highly contractile (Fig. 9b, c), and partially covered by the sponge (Fig. 10d). Five or six oral capitate tentacles up to 200 μm long (capitula ~60 μm wide) and 9–12 aboral tentacles up to 180 μm long and with smaller capitula (capitula ~45 μm wide). Capitula containing stenoteles of two size classes. Polyps with a proximal ring of macrobasic apotrichous euryteles (Fig. 10e) corresponding to the point where the sponge stops surrounding the polyps, approximately at one-third of the polyp body. Up to four medusa buds borne basally, kept inside a tissue pocket protected externally by the ring of euryteles (Fig. 10e) and covered by the sponge. Medusa buds exposed only at maturation, before release. Newly liberated medusa (Fig. 9f, g) with a bell-shaped umbrella (~750 μm high and ~800 μm wide), manubrium extending for one-third or half of the umbrella (Fig. 10g), and microbasic euryteles scattered on the exumbrella. Four perradial canals ending in two triangular tentaculate bulbs and two smaller atentaculate bulbs (Fig. 9g, h). Atentaculate bulbs with an exumbrellar cnidocyst pouch containing up to five euryteles, and in some cases small-sized stenoteles (Fig. 10i). Euryteles found also in tentaculate bulbs (Fig. 10h). Tentacular bubs bearing one tentacle each, about 700 μm long, with 50–100 rounded ciliated cnidophores approximately 30 μm wide, armed with 3–4 bean-shaped macrobasic apotrichous euryteles. Seven days old medusa with similar size and longer tentacles (up to 2 mm) equipped with more cnidophores. Living polyps transparent (Fig. 9c, d), sometimes with a reddish gastroderm and living medusae transparent, with reddish bulbs and a whitish manubrium (Fig. 10f).

Cnidome: Small stenoteles (5–7 × 4–5 μm) and large stenoteles (10–13 × 8–11 μm) in capitula (Fig. 10j). Macrobasic apotrichous euryteles in a ring at the base of polyps, in clusters in hydrorhiza, in exumbrellar pouches, and in bulbs (23–29 × 15–21 μm; discharged shaft: 460–500 μm) (Fig. 9i, k, l). Bean-shaped macrobasic apotrichous euryteles in cnidophores (6–8 × 4–6 μm; discharged shaft: 48–54 μm) (Fig. 10m). Microbasic euryteles on exumbrella (8–11 × 6–9 μm; discharged shaft: 19–21 μm) (Fig. 10n).

Discussion

An updated phylogeny of the Cladocorynidae

In this work, a phylogenetic hypothesis of the family Cladocorynidae was proposed and, according to multiple lines of evidence, the new genus *Pseudozanclea* was established to accommodate *Zanclea timida*. Various phylogenetic analyses consistently placed *Pseudozanclea timida* as the sister group of *Pteroclava* and as phylogenetically distant from other *Zanclea* species. The description, for the first time, of the newly released medusa of *P. timida* demonstrated that there are strong similarities between the *Pseudozanclea* and *Pteroclava* medusae, both in the general morphology

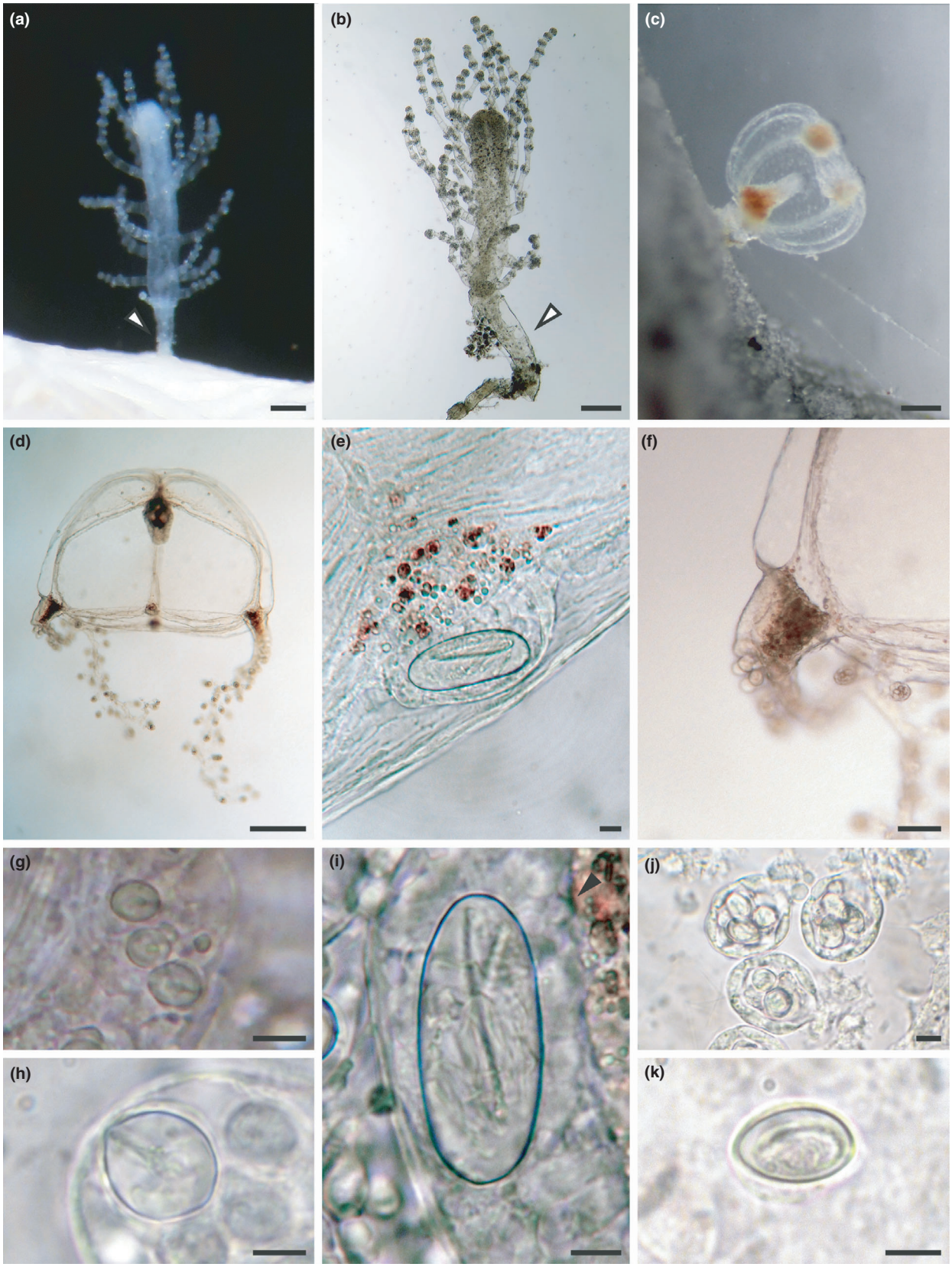
(a)
(b)
(c)
(d)
(e)
(f)
(g)
(i)
(j)
(h)
(k)

Fig. 9. *Pteroclava krempfi*. (a, b) Polyps showing moniliform tentacles and a perisarc-covered pedicel (arrowheads). (c) Polyp with a mature medusa bud, showing reproductive exhaustion. (d) Newly released medusa. (e) Exumbrellar cnidocyst pouch with an eurytele. (f) Tentaculate bulb. (g) Small stenoteles. (h) Large stenotele. (i) Macrobasic apotrichous eurytele. (j) Cnidophores with bean-shaped macrobasic apotrichous euryteles. (k) Microbasic eurytele. Scale bars: (a–d) 0.2 mm; (e, g–k) 5 μm; (f) 50 μm.

and in the unique presence of exumbrellar cnidocyst pouches containing euryteles. The polyp stage also shares a similarity with those of other cladocorynid taxa, which is the presence of macrobasic apotrichous euryteles organized in a specific pattern. Finally, similarly to *Pteroclava*, *Pseudozanclea* is an obligate symbiont of octocorals.

The family Cladocorynidae was initially erected to accommodate the genus *Cladocoryne* (Allman, 1872), whereas only later Petersen (1990) and Boero et al., (1995) proposed to include the genus *Pteroclava*. This conclusion was justified by the synapomorphy represented by the presence of patches of large macrobasic euryteles in the polyp stages of both genera. However, similar patches are found at least in another non-cladocorynid species, *Eudendrium glomeratum* Picard, 1952, in which patches can form an irregular band (Schuchert, 2008). The presence of eurytele patches in Cladocorynidae and *E. glomeratum* clearly represents morphological convergence, with the trait emerging twice independently in two phylogenetically distant suborders (Maronna et al., 2016). As demonstrated in this work, *Pseudozanclea timida* shows aggregations of macrobasic euryteles in the polyp stage, even if organized in a ring rather than patches, and this organization may derive from the coalescence of the patches observed in *Pteroclava* and *Cladocoryne*. Interestingly, specimens from Indonesia and associated with *Paratelesto* possess macrobasic apotrichous mastigophores instead of euryteles, even if the heteronemes of the two populations show similarity in shape and overlap in size. Maldivian heteronemes have an enlargement of the distal part of the shaft, typical of euryteles, and similar to that occurring in *Pteroclava* and *Cladocoryne,* i.e., with a zig-zag pattern and covered with spines (see for instance Maggioni et al., 2016: 488, Fig. 7 and Bouillon et al., 1987: 283: Fig. 7). On the other hand, the shaft figured by Puce et al. (2008b: 1652: Fig. 7g) appears to be the same diameter for all its length, a typical feature of mastigophores. This could be the case, but it is noteworthy that the figured distal portion of the shaft seems damaged, for instance with spines not covering the end of the shaft, and this may have caused an incorrect classification of the cnidocyst occurring in Indonesian specimens.

Whatever the cnidocyst type found in the ring, the function may relate to the polyp defence, since *P. timida* hydroids are able to retract within their basal cup, exposing only the cnidocyst ring and the tentacular capitula (Puce et al., 2008b). Moreover, the immature medusa buds are kept inside a tissue pocket below the cnidocyst ring, and the latter may provide protection to developing medusae. *Pseudozanclea timida* has stolonal cnidocyst clusters, which have been hypothesized to protect the perisarc-derived stolons from predators (Puce et al., 2008b). However, the stolons of Maldivian specimens were always covered by a sponge, contrary to those described from Indonesia. Therefore, the defensive function of stolonal cnidocyst clusters does not seem to apply for the Maldivian specimens of *P. timida*. The associated sponge also covers the proximal portion of *P. timida* hydranths, including the medusa buds, and this may result in a further protection of the immature medusae before release (Maggioni et al., 2020a). The sponge was never observed to cover *P. timida* polyps above the cnidocyst ring, and the aggregation of euryteles may prevent an excessive overgrowth of the hydroids by the sponge.

Another synapomorphy of the family is the presence of exumbrellar pouches with eurytele capsules, a peculiarity never found in other hydrozoan species. The medusae of both *Pseudozanclea timida* and *Pteroclava krempfi* clearly possess this feature on atentaculate bulbs. *Cladocoryne* species also show exumbrellar eurytele aggregations on their cryptomedusoids. The presence of these exumbrellar cnidocyst clusters was confirmed herein for both *C. floccosa* and *C. haddoni*, and are apparently present also in *C. minuta* (Watson, 2005), even if described as scattered rather than grouped. Regarding the other two *Cladocoryne* species, the reproductive structures of *C. travancorensis* are unknown, whereas the cnidome of the *C. littoralis* cryptomedusoids was not reported in the original description (Mammen, 1963). It is therefore likely that the exumbrellar cnidocyst pouches containing euryteles are found in all cladocorynid species, but future reanalysis of the poorly described species will be necessary to address this issue.

The clade *Pseudozanclea* + *Pteroclava* is composed of obligate octocoral symbionts, and this association is likely to have arisen in the MRCA of the two genera. The species *Pteroclava crassa* was described growing on the hydroid *Macrorhynchia philippina* Kirchenpauer, 1872 (Pictet, 1893), but the information on this species is very scant and the only difference with *P. krempfi* appears to be the host. Therefore, it remains unclear whether the two *Pteroclava* species are conspecific or not. Within the superfamily Zancleida,

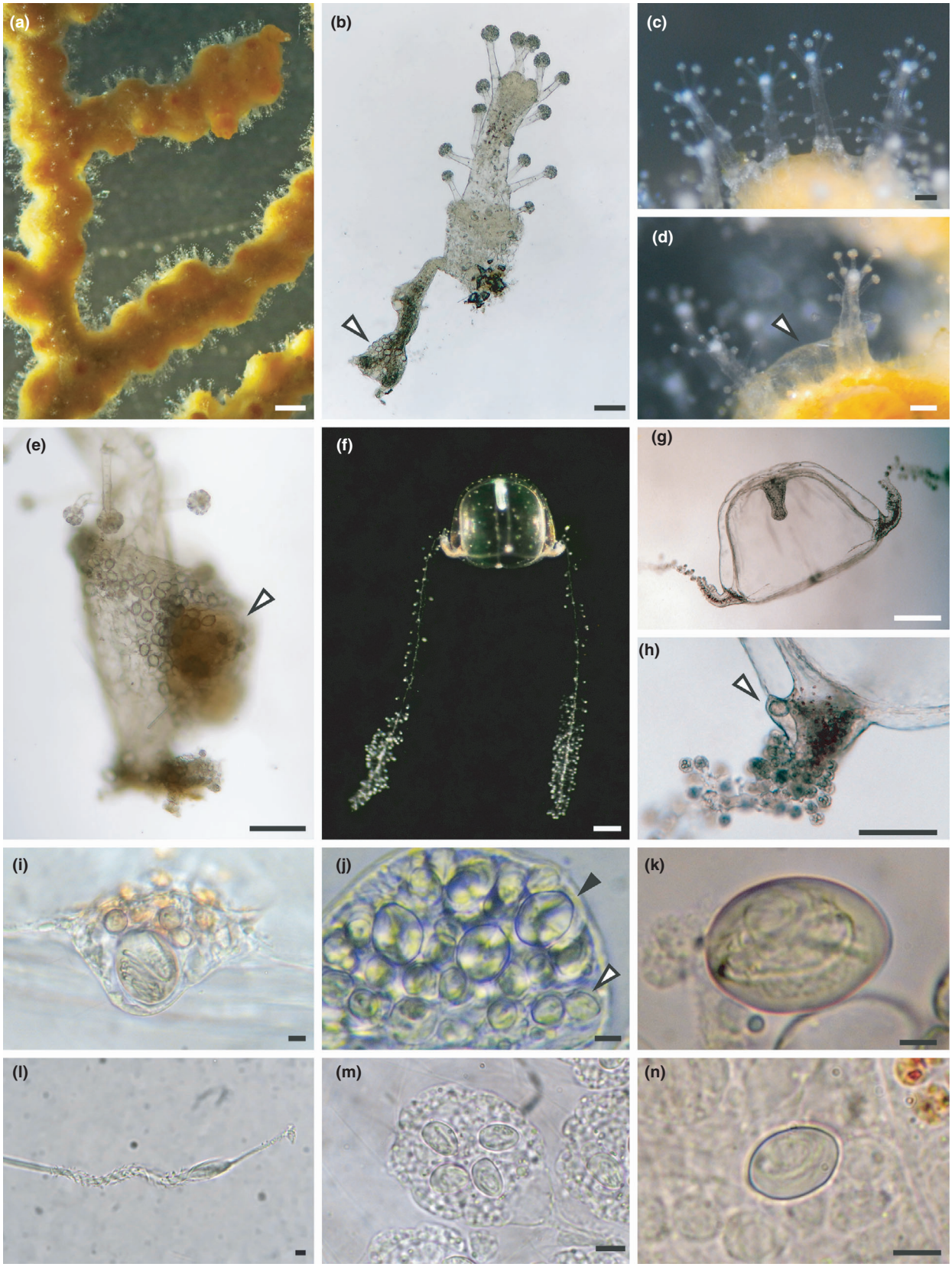
(a)
(b)
(c)
(d)
(e)
(f)
(g)
(h)
(i)
(j)
(k)
(l)
(m)
(n)

Fig. 10. *Pseudozanclea timida*. (a) Living colony growing on *Bebryce* cf. *grandicalyx*. (b) Polyp with a portion of the hydrorhiza showing an eurytele cluster (arrowhead). (c, d) Living polyps partially overgrown by a sponge in the family Suberitidae (arrowhead). (e) Medusa buds (arrowhead) surrounded by polyp tissue equipped with eurytele capsules arranged in a ring. (f, g) Newly released medusa. (h) Tentacular bulb with an eurytele (arrowhead). (i) Exumbrellar cnidocyst pouch with an eurytele and stenoteles. (j) Small stenoteles (white arrowhead) and large stenoteles (black arrowhead). (k) Macrobasic apotrichous eurytele. (l) Terminal portion of the shaft of the macrobasic apotrichous eurytele. (m) Cnidophore with bean-shaped macrobasic apotrichous euryteles. (n) Microbasic eurytele. Scale bars: (a) 2 mm; (b, e, h) 100 μm; (c, d, f–g) 0.2 μm; (i–n) 5 μm.

another species was described growing on octocorals, *Zanclea cubensis* Varela, 2012, described from the Caribbean Sea (Varela, 2012). *Zanclea cubensis* is very similar to other zancleid species, having a claviform hydranth with oral and aboral capitate tentacles, and stenoteles and euryteles as cnidocysts. The medusa was not described, and the species was named mostly based on the combination of the type of euryteles (macrobasic holotrichous) and the association with octocorals. Considering the lack of genetic data and the partial description of the species, along with the polyphyletic nature of the family Zancleidae and the genus *Zanclea* (Maggioni et al., 2018), the phylogenetic position of *Z. cubensis* remains unknown. Therefore, it is currently not possible to establish how many times the association with octocorals evolved in the Zancleida.

Taxonomic uncertainties in the Cladocorynidae

Previous studies suggested the presence of three cryptic species within *Pteroclava krempfi*, based on the analysis of four DNA regions of Maldivian and Caribbean samples (Maggioni et al., 2016; Montano et al., 2017). In the present work, several colonies associated with multiple hosts and from different localities were analyzed to better comprehend the genetic structure of the *P. krempfi* species complex. Despite the conserved general morphology across samples, our phylogenetic, genetic distance, and single- and multi-locus species delimitation analyses confirmed the presence of highly divergent genetic lineages. The number of possible species hypotheses varied according to the method used and DNA region analyzed, with mitochondrial and multi-locus analyses resulting in the highest numbers of species hypotheses. The higher number of species found based on mitochondrial regions is concordant with the higher rates of nucleotide substitution found in mitochondrial DNA of hydrozoans compared to other phylogenetically informative nuclear regions (e.g., Maggioni et al., 2020b, c). It therefore remains unclear how many possible species exist under the name *P. krempfi*, also because clades Ib and IIb are herein represented by a limited number of samples. Unfortunately, it is currently not possible to formally describe the clades due to the lack of *P. krempfi* material suitable for genetic analyses from the type locality (Vietnam) and associated with the type's host (*Cladiella krempfi*). Additionally, *Cladocoryne floccosa* may be another species complex, given the high intraspecific genetic distances found in this study for all mitochondrial and some nuclear regions. *Cladocoryne floccosa* has a wide distribution, from tropical to temperate areas (Schuchert, 2006; Gravili et al., 2015), and only a thorough sampling across the whole geographic range and an accurate morpho-molecular assessment would clarify the possible presence of cryptic lineages or species.

The analysis of cnidocyst size data of *P. krempfi* revealed partial differences among the genetic clades, since a clear size variation was found only for euryteles, showing a larger size in organisms from the Caribbean (clade III). However, no differences were detected in eurytele size between clade Ia and IIa and stenotele size among all clades. The statistical treatment of cnidocyst size data was previously used to search for fine-scale variations in other hydrozoan species, revealing in some cases no differences (Wollschlager et al., 2013) or significant differences among genetic clades (Arrigoni et al., 2018; Manca et al., 2019; Maggioni et al., 2020c). Similar studies were performed also on sea anemones, in which only some cnidocysts, coming from particular structures, varied among morphs (González-Muñoz et al., 2017), or did not vary at all (González-Muñoz et al., 2018), showing a high intraspecific variability (Garese et al., 2016). The results obtained in this work are therefore in line with previous works showing limited, but in some cases still useful, power of discrimination of cnidocyst size among closely related species or populations. Nevertheless, to present, there is no evidence that can explain the intraspecific variation on cnidocysts.

The obtained *P. krempfi* clades showed different host preferences. Clades Ia and IIb showed overlapping host octocoral genera, and all clade I colonies but one were found living on genera belonging to the family Alcyoniidae. The only exception was a colony found on *Paralemnalia* (family Nephtheidae). No host overlapping was found between clade I and II at the genus level, with a single exception at the family level being a clade IIa colony associated with *Dendronephthya*, another genus of the family Nephtheidae. All other clade II colonies were associated with several octocoral genera and families, and no host overlapping between clades IIa and IIb was observed at both the genus and family level, even if clade IIb is currently composed of a single colony. Finally, clade III was

consistently found associated with *Antillogorgia* (Montano et al., 2017; Miglietta et al., 2018). Another *P. krempfi* record from the Caribbean Sea reports a colony associated with *Plexaurella grisea* Kunze, 1916 (Varela and Cabrales Caballero, 2010), suggesting a wider host range for clade III. Overall, a certain degree of host specificity can be detected, mostly at the family level, even if with some exceptions. Host specificity has recently been demonstrated for several other coral-reef invertebrates associated with a variety of benthic organisms, such as parasitic gastropods (Gittenberger and Gittenberger, 2011; Gittenberger and Hoeksema, 2013; Potkamp et al., 2017; Fritts-Penniman et al., 2020), coral-dwelling barnacles (Malay and Michonneau, 2014; Tsang et al., 2014), commensal shrimps (Horká et al., 2016), copepods (Korzhavina et al., 2019), benthic ctenophores (Alamaru et al., 2017), coral gall-crabs (García-Hernández et al., 2020), acoel flatworms (Kunihiro et al., 2019), and hydrozoans (Maggioni et al., 2020b, c). Host-specificity of associated species can be very weak as observed in various coral-dwelling copepods living on mushroom corals (Ivanenko et al., 2018) and in one serpulid worm living on a wide range of Caribbean scleractinians (Hoeksema and Hove, 2017). Hence, the causes (and consequences) of these, more or less specific, associations largely remain unclear and need further research. Additionally, colonies belonging to the same clade (clade I) displayed variable host preference, with some Alcyoniidae genera showing higher prevalence of the symbiosis, and these prevalences also varied according to the studied locality and reef type (Montano et al., 2017; Seveso et al., 2020). Therefore, despite a single clade being associated with multiple octocoral genera, it is likely that, at least in some localities, some of the associations are rarer than others, or even occasional, and that the association is host-reliant (Montano et al., 2017).

In conclusion, this work sheds new light on the evolution and diversity of the poorly known family Cladocorynidae, providing a new well-supported phylogenetic reconstruction of the family, establishing a new genus, and demonstrating the presence of several DNA-based species hypotheses. Moreover, the new data on the host specificity and geographic distribution of *P. krempfi* provide valuable insights for future research on how the current diversity patterns have evolved and on the study of the nature of the hydrozoan-octocoral symbioses.

Acknowledgements

The authors thank all the people involved in collecting/providing material or organising sampling campaigns: Peter Schuchert (MHNG, Switzerland), Tullia Isotta Terraneo (KAUST, Saudi Arabia), Malek Amr Gusti (KAUST, Saudi Arabia), Timothy Ravasi (OIST, Japan), the captain and crew of the MV Dream-Master (Saudi Arabia), the KAUST Coastal and Marine Resources Core Lab, Inga Dehnert (UNIMIB, Italy), Nicholas WL Yap (NUS, Singapore), Sudhanshi S Jain (NUS, Singapore), Stephen Keable (Australian Museum), Penny Berents (Australian Museum), Anne Hoggett (Australian Museum), Lyle Vail (Australian Museum). Additionally, we wish to thank Leen P. van Ofwegen (Naturalis, The Netherlands) for his valuable help in identifying the octocoral *Paralemnalia* sp., Peter Schuchert for his comments on an earlier version of the manuscript, and two anonymous referees for their thorough revision of this work. Permissions relevant to undertake the research have been obtained from the applicable governmental agencies. Fieldwork at St. Eustatius was funded through a Martin Fellowship from Naturalis Biodiversity Center to SM, while logistic support was supplied by St. Eustatius Marine Parks (STENAPA), the Caribbean Netherlands Science Institute (CNSI) and Scubaqua Dive Centre. Samples from Eilat (Israel) were collected during the HyDRa Project funded by the EU FP7 Research Infrastructure Initiative 'ASSEMBLE' (Grant #227799) to DP. Financial support to DP for collecting samples at Lizard Island (Australia) was provided by the 2018 John and Laurine Proud Fellowship and the Australian Museum's Lizard Island Research Station. Fieldwork in Mozambique was conducted during the Green Bubbles financed by EU's H2020 research and innovation programme to DP, under the Marie Sklodowska-Curie grant agreement no 643712 (Permit n° 09/2018 ANAC). Fieldwork in Singapore was partially funded by the National Research Foundation, Prime Minister's Office, Singapore under its Marine Science R&D Programme (MSRDP-P03) to DH.

Conflict of interest

None declared.

References

Ainsworth, T.D., Renzi, J.J. & Silliman, B.R., 2020. Positive interactions in the coral macro and microbiome. Trends Microbiol. 8, 602–604.

Alamaru, A., Hoeksema, B.W., Van Der Meij, S.E.T. & Huchon, D., 2017. Molecular diversity of benthic ctenophores (Coeloplanidae). Sci. Rep. 7, 6365.

Allman, G.J., 1872. A Monograph of the Gymnoblastic Or Tubularian Hydroids: The Genera and Species of the Gymnoblasta. Ray Society, London, UK.

Antokhina, T.I. & Britayev, T.A., 2012. Sea stars and their macrosymbionts in the Bay Of Nhatrang, Southern Vietnam. Paleontol. J. 46, 894–908.

Arrigoni, R., Maggioni, D., Montano, S., Hoeksema, B.W., Seveso, D., Shlesinger, T., Terraneo, T.I., Tietbohl, M.D. & Berumen, M.L., 2018. An integrated morpho-molecular approach to delineate species boundaries of *Millepora* from the Red Sea. Coral Reefs 37, 967–984.

Bates, D., Mächler, M., Bolker, B. & Walker, S., 2015. Fitting linear mixed-effects models using lme4. J. Stat Softw. 67, 1–48.

Billard, A., 1919. Note sur une espèce nouvelle d'hydroïde gymnoblastique (*Clava krempfi*), parasite d'un Alcyonaire. Bull. Mus. Nat. Hist. 3, 187–188.

Bo, M., Di Camillo, C.G., Puce, S., Canese, S., Giusti, M., Angiolillo, M. & Bavestrello, G., 2011. A tubulariid hydroid associated with anthozoan corals in the Mediterranean Sea. Ital. J. Zool. 78, 487–496.

Boero, F., Bouillon, J. & Bonnet, G., 1995. The life cycle of *Pteroclava krempfi* (Cnidaria, Hydrozoa, Cladocorynidae), with notes on *Asyncoryne philippina* (Asyncorynidae). Sci. Mar. 59, 65–76.

Bouckaert, R., Heled, J., Kühnert, D., Vaughan, T., Wu, C.H., Xie, D., Suchard, M.A., Rambaut, A. & Drummond, A.J., 2014. BEAST 2: a software platform for Bayesian evolutionary analysis. PLoS Comput. Biol. 10, e1003537.

Bouillon, J., Boero, F. & Seghers, G., 1987. Redescription of *Cladocoryne haddoni* Kirkpatrick and a proposed phylogeny of the superfamily Zancleoidea (Anthomedusae, Hydrozoa, Cnidaria). Indo-Malayan Zool. 4, 279–292.

Bouillon, J., Gravili, C., Gili, J.M. & Boero, F., 2006. An Introduction to Hydrozoa. Publications Scientifiques du Museum, Paris, France.

Castresana, J., 2000. Selection of conserved blocks from multiple alignments for their use in phylogenetic analysis. Mol. Biol. Evol. 17, 540–552.

Darriba, D., Taboada, G.L., Doallo, R. & Posada, D., 2012. jModelTest 2: more models, new heuristics and parallel computing. Nat. Methods 9, 772.

Drummond, A.J., Suchard, M.A., Xie, D. & Rambaut, A., 2012. Bayesian phylogenetics with BEAUti and the BEAST 1.7. Mol. Biol. Evol. 29, 1969–1973.

Ezard, T., Fujisawa, T. & Barraclough, T.G., 2009. SPLITS: Species limits by threshold statistics. R Package Version 1.0-11. http://r-forge.r-project.org/projects/splits/

Fabricius, K.E. & Alderslade, P., 2001. Soft Corals and Sea Fans: A Comprehensive Guide to the Tropical Shallow Water Genera of the Central-West Pacific, the Indian Ocean and the Red Sea. Australian Institute of Marine Science (AIMS), Townsville, Australia.

Fox, J. & Bouchet-Valat, M., 2020. Rcmdr: R Commander. R package version 2.7-1. https://socialsciences.mcmaster.ca/jfox/Misc/Rcmdr/

Fritts-Penniman, A.L., Gosliner, T.M., Mahardika, G.N. & Barber, P.H., 2020. Cryptic ecological and geographic diversification in coral-associated nudibranchs. Mol. Phylogenet. Evol. 144, 106698.

Fujisawa, T. & Barraclough, T.G., 2013. Delimiting species using single-locus data and the Generalized Mixed Yule Coalescent approach: a revised method and evaluation on simulated data sets. Syst. Biol. 62, 707–724.

García-Hernández, J.E., De Gier, W., Van Moorsel, G.W.N.M. & Hoeksema, B.W., 2020. The scleractinian *Agaricia undata* as a new host for the Caribbean coral gall crab *Opecarcinus hypostegus* at Bonaire, southern Caribbean. Symbiosis 81, 303–311.

García-Hernández, J.E., Hammerman, N.M., Cruz-Motta, J.J. & Schizas, N.V., 2019. Associated organisms inhabiting the calcareous sponge *Clathrina lutea* in La Parguera, Puerto Rico. Caribb. J. Sci. 49, 239–254.

Garese, A., Carrizo, S. & Acuña, F.H., 2016. Biometry of sea anemone and corallimorpharian cnidae: statistical distribution and suitable tools for analysis. Zoomorphology 135, 395–404.

Gates, R.D. & Ainsworth, T.D., 2011. The nature and taxonomic composition of coral symbiomes as drivers of performance limits in scleractinian corals. J. Exp. Mar. Biol. Ecol. 408, 94–101.

Gittenberger, A. & Gittenberger, E., 2011. Cryptic, adaptive radiation of endoparasitic snails: sibling species of *Leptoconchus* (Gastropoda: Coralliophilidae) in corals. Org. Divers. Evol. 11, 21–41.

Gittenberger, A. & Hoeksema, B.W., 2013. Habitat preferences of coral-associated wentletrap snails (Gastropoda: Epitoniidae). Contrib. Zool. 82, 1–25.

Goh, N.K., Ng, P.K. & Chou, L.M., 1999. Notes on the shallow water gorgonian-associated fauna on coral reefs in Singapore. Bull. Mar. Sci. 65, 259–282.

González-Muñoz, R., Garese, A., Tello-Musi, J.L. & Acuña, F.H., 2017. Morphological variability of the "Caribbean hidden anemone" *Lebrunia coralligens* (Wilson, 1890). Zoomorphology 136, 287–297.

González-Muñoz, R., Hernández-Ortiz, C., Garese, A., Simões, N. & Acuña, F.H., 2018. Comparison of cnidae sizes between the two morphotypes of the giant Caribbean sea anemone *Condylactis gigantea* (Actiniaria: Actiniidae). Rev. Biol. Trop. 66, 1055–1064.

Gravili, C., De Vito, D., Di Camillo, C.G., Martell, L., Piraino, S. & Boero, F., 2015. The non-Siphonophoran Hydrozoa (Cnidaria) of Salento, Italy with notes on their life-cycles: an illustrated guide. Zootaxa 3908, 1–187.

Heled, J. & Drummond, A.J., 2009. Bayesian inference of species trees from multilocus data. Mol. Biol. Evol. 27, 570–580.

Hoeksema, B.W., Van Beusekom, M., Ten Hove, H.A., Ivanenko, V.N., Van Der Meij, S.E.T. & Van Moorsel, G.W.N.M., 2017. *Helioseris cucullata* as a host coral at St. Eustatius. Dutch Caribbean. Mar. Biodivers. 47, 71–78.

Hoeksema, B.W. & Ten Hove, H.A., 2017. The invasive sun coral *Tubastraea coccinea* hosting a native Christmas tree worm at Curaçao, Dutch Caribbean. Mar. Biodivers. 47, 59–65.

Hoeksema, B.W., Lau, Y.W. & Ten Hove, H.A., 2015. Octocorals as secondary hosts for Christmas tree worms at Curaçao. Bull. Mar. Sci. 91, 489–490.

Hoeksema, B.W., Van Der Meij, S.E.T. & Fransen, C.H.J.M., 2012. The mushroom coral as a habitat. J. Mar. Biol. Assoc. U.K. 92, 647–663.

Horká, I., De Grave, S., Fransen, C.H., Petrusek, A. & Ďuriš, Z., 2016. Multiple host switching events shape the evolution of symbiotic palaemonid shrimps (Crustacea: Decapoda). Sci. Rep., 6, 26486.

Huelsenbeck, J.P., Nielsen, R. & Bollback, J.P., 2003. Stochastic mapping of morphological characters. Syst. Biol. 52, 131–158.

Ivanenko, V.N., Hoeksema, B.W., Mudrova, S.V., Nikitin, M.A., Martínez, A., Rimskaya-Korsakova, N.N., Berumen, M.L. & Fontaneto, D., 2018. Lack of host specificity of copepod crustaceans associated with mushroom corals in the Red Sea. Mol. Phylogenet. Evol. 127, 770–780.

Kapli, P., Lutteropp, S., Zhang, J., Kobert, K., Pavlidis, P., Stamatakis, A. & Flouri, T., 2017. Multi-rate Poisson tree processes for single-locus species delimitation under maximum likelihood and Markov chain Monte Carlo. Bioinformatics 33, 1630–1638.

Katoh, K. & Standley, D.M., 2013. MAFFT multiple sequence alignment software version 7: improvements in performance and usability. Mol. Biol. Evol. 30, 772–780.

Korzhavina, O.A., Hoeksema, B.W. & Ivanenko, V.N., 2019. A review of Caribbean Copepoda associated with reef-dwelling cnidarians, echinoderms and sponges. Contrib. Zool. 88, 297–349.

Kühn, A.L. & Haase, M., 2020. QUIDDICH: QUick IDentification of DIagnostic CHaracters. J. Zool. Syst. Evol. Res. 58, 22–26.

Kumar, S., Stecher, G., Li, M., Knyaz, C. & Tamura, K., 2018. MEGA X: molecular evolutionary genetics analysis across computing platforms. Mol. Biol. Evol. 35, 1547–1549.

Kunihiro, S., Farenzena, Z., Hoeksema, B.W., Groenenberg, D.S.J., Hermanto, B. & Reimer, J.D., 2019. Morphological and phylogenetic diversity of *Waminoa* and similar flatworms (Acoelomorpha) in the western Pacific Ocean. Zoology, 136, 125692.

Kuznetsova, A., Brockhoff, P.B. & Christensen, R.H.B., 2017. lmerTest package: tests in linear mixed effects models. J. Stat. Softw. 82, 1–26.
Lanfear, R., Calcott, B., Ho, S.Y. & Guindon, S., 2012. PartitionFinder: combined selection of partitioning schemes and substitution models for phylogenetic analyses. Mol. Biol. Evol. 29, 1695–1701.
Leaché, A.D. & Fujita, M.K., 2010. Bayesian species delimitation in West African forest geckos (*Hemidactylus fasciatus*). Proc. Roy. Soc. B-Biol. Sci. 277, 3071–3077.
Leigh, J.W. & Bryant, D., 2015. popart: full-feature software for haplotype network construction. Methods Ecol. Evol. 6, 1110–1111.
Maddison, W.P. & Maddison, D.R., 2006. Mesquite: a modular system for evolutionary analysis. http://www.mesquiteproject.org
Maggioni, D., Arrigoni, R., Galli, P., Berumen, M.L., Seveso, D. & Montano, S., 2018. Polyphyly of the genus *Zanclea* and family Zancleidae (Hydrozoa, Capitata) revealed by the integrative analysis of two bryozoan-associated species. Contrib. Zool. 87, 87–104.
Maggioni, D., Arrigoni, R., Seveso, D., Galli, P., Berumen, M.L., Denis, V., Hoeksema, B.W., Huang, D., Manca, F., Pica, D., Puce, S., Reimer, J.D. & Montano, S., 2020b. Evolution and biogeography of the *Zanclea*-Scleractinia symbiosis. Coral Reefs, https://doi.org/10.1007/s00338-020-02010-9.
Maggioni, D., Galli, P., Berumen, M.L., Arrigoni, R., Seveso, D. & Montano, S., 2017. *Astrocoryne cabela*, gen. nov. et sp. nov. (Hydrozoa: Sphaerocorynidae), a new sponge-associated hydrozoan. Invertebr. Syst. 31, 734–746.
Maggioni, D., Montano, S., Seveso, D. & Galli, P., 2016. Molecular evidence for cryptic species in *Pteroclava krempfi* (Hydrozoa, Cladocorynidae) living in association with alcyonaceans. Syst. Biodivers. 14, 484–493.
Maggioni, D., Montano, S., Voigt, O., Seveso, D. & Galli, P., 2020a. A mesophotic hotel: the octocoral *Bebryce* cf. *grandicalyx* as a host. Ecology, 101, e02950.
Maggioni, D., Schiavo, A., Ostrovsky, A.N., Seveso, D., Galli, P., Arrigoni, R., Berumen, M.L., Benzoni, F. & Montano, S., 2020c. Cryptic species and host specificity in the bryozoan-associated hydrozoan *Zanclea divergens* (Hydrozoa, Zancleidae). Mol. Phylogenet. Evol. 151, 106893.
Malay, M.C.D. & Michonneau, F., 2014. Phylogenetics and morphological evolution of coral-dwelling barnacles (Balanomorpha: Pyrgomatidae). Biol. J. Linn. Soc. 113, 162–179.
Mammen, T.A., 1963. On a collection of hydroids from South India. I. Suborder Athecata. J. Mar. Biol. Assoc. India 5, 27–61.
Manca, F., Puce, S., Caragnano, A., Maggioni, D., Pica, D., Seveso, D., Galli, P. & Montano, S., 2019. Symbiont footprints highlight the diversity of scleractinian-associated *Zanclea* hydrozoans (Cnidaria, Hydrozoa). Zool. Scr. 48, 399–410.
Maronna, M.M., Miranda, T.P., Peña-Cantero, Á.L., Barbeitos, M.S. & Marques, A.C., 2016. Towards a phylogenetic classification of Leptothecata (Cnidaria, Hydrozoa). Sci. Rep. 6, 18075.
Miglietta, M.P., Piraino, S., Pruski, S., Alpizar Gonzalez, M., Castellanos-Iglesias, S., Jerónimo-Aguilar, S., Lawley, J.W., Maggioni, D., Martell, L., Matsumoto, Y., Moncada, A., Nagale, P., Phongphattarawat, S., Sheridan, C., Soto Àngel, J.J., Sukhoputova, A. & Collin, R., 2018. An integrative identification guide to the Hydrozoa (Cnidaria) of Bocas del Toro. Panama. Neotrop. Biodivers. 4, 103–113.
Miller, M.A., Pfeiffer, W. & Schwartz, T., 2010. Creating the CIPRES Science Gateway for inference of large phylogenetic trees. In: Proceedings of the Gateway Computing Environments Workshop.
Montano, S., 2020. The extraordinary importance of coral-associated fauna. Diversity 12, 357.
Montano, S., Maggioni, D., Galli, P. & Hoeksema, B.W., 2017. A cryptic species in the *Pteroclava krempfi* species complex (Hydrozoa, Cladocorynidae) revealed in the Caribbean. Mar. Biodivers. 47, 83–89.
Neo, M.L., Eckman, W., Vicentuan, K., Teo, S.-L.-M. & Todd, P.A., 2015. The ecological significance of giant clams in coral reef ecosystems. Biol. Conserv. 181, 111–123.
Paradis, E., Claude, J. & Strimmer, K., 2004. APE: analyses of phylogenetics and evolution in R language. Bioinformatics 20, 289–290.
Petersen, K.W. (1990) Evolution and taxonomy in capitate hydroids and medusae (Cnidaria: Hydrozoa). Zool. J. Linnean Soc., 100, 101–231.
Pictet, C., 1893. Étude sur les hydraires de la Baie d'Amboine. Rev. Suisse Zool. 1, 1–64.
Pons, J., Barraclough, T.G., Gomez-Zurita, J., Cardoso, A., Duran, D.P., Hazell, S., Kamoun, S., Sumlin, W.D. & Vogler, A.P., 2006. Sequence based species delimitation for the DNA taxonomy of undescribed insects. Syst. Biol. 55, 595–609.
Potkamp, G., Vermeij, M.J. & Hoeksema, B.W., 2017. Genetic and morphological variation in corallivorous snails (*Coralliophila* spp.) living on different host corals at Curaçao, southern Caribbean. Contr. Zool. 86, 111–S9.
Puce, S., Di Camillo, C.G. & Bavestrello, G., 2008b. Hydroids symbiotic with octocorals from the Sulawesi Sea, Indonesia. Mar. Biol. Assoc. U.K. 88, 1643–1654.
Puce, S., Cerrano, C., Di Camillo, C.G. & Bavestrello, G., 2008a. Hydroidomedusae (Cnidaria: Hydrozoa) symbiotic radiation. J. Mar. Biol. Assoc. U.K. 88, 1715–1721.
Puillandre, N., Brouillet, S. & Achaz, G., 2020. ASAP: assemble species by automatic partitioning. Mol. Ecol. Res. 21, 609–620.
Puillandre, N., Lambert, A., Brouillet, S. & Achaz, G., 2012. ABGD, Automatic Barcode Gap Discovery for primary species delimitation. Mol. Ecol. 21, 1864–1877.
R Core Team, 2020. R: A Language and Environment for Statistical Computing. R Foundation for Statistical Computing, Vienna, Austria.
Rambaut, A., Suchard, M.A., Xie, D. & Drummond, A.J., 2014. Tracer v1.6. http://beast.bio.ed.ac.uk/Tracer/
Reid, N.M. & Carstens, B.C., 2012. Phylogenetic estimation error can decrease the accuracy of species delimitation: a Bayesian implementation of the general mixed Yule-coalescent model. BMC Evol. Biol. 12, 196.
Revell, L.J., 2012. phytools: an R package for phylogenetic comparative biology (and other things). Methods Ecol. Evol. 3, 217–223.
Ronquist, F., Teslenko, M., van der Mark, P., Ayres, D.L., Darling, A., Höhna, S., Larget, B., Liu, L., Suchard, M.A. & Huelsenbeck, J.P., 2012. MrBayes 3.2: efficient Bayesian phylogenetic inference and model choice across a large model space. Syst. Biol. 61, 539–542.
Rozas, J., Ferrer-Mata, A., Sánchez-DelBarrio, J.C., Guirao-Rico, S., Librado, P., Ramos-Onsins, S.E. & Sánchez-Gracia, A., 2017. DnaSP 6: DNA sequence polymorphism analysis of large datasets. Mol. Biol. Evol. 34, 3299–3302.
Russel, F.S., 1953. The medusae of the British Isles. Cambridge University Press, London, UK.
Schönberg, C.H.L., Hosie, A.M., Fromont, J., Marsh, L. & O'Hara, T., 2015. Apartment-style living on a kebab sponge. Mar. Biodivers. 46, 331–332.
Schuchert, P., 2003. Hydroids (Cnidaria, Hydrozoa) of the Danish expedition to the Kei Islands. Steenstrupia 27, 137–256.
Schuchert, P., 2006. The European athecate hydroids and their medusae (Hydrozoa, Cnidaria): Capitata part 1. Rev. Suisse Zool. 113, 325–410.
Schuchert, P., 2008. The European athecate hydroids and their medusae (Hydrozoa, Cnidaria): Filifera part 4. Rev. Suisse Zool. 115, 677–757.
Seveso, D., Maggioni, D., Arrigoni, R., Montalbetti, E., Berumen, M.L., Galli, P. & Montano, S., 2020. Environmental gradients and host availability affecting the symbiosis between *Pteroclava krempfi* and alcyonaceans in the Saudi Arabian central Red Sea. Mar. Ecol. Prog. Ser. 653, 91–103.
Seveso, D., Montano, S., Pica, D., Maggioni, D., Galli, P., Allevi, V., Bastari, A. & Puce, S., 2016. *Pteroclava krempfi*-octocoral

symbiosis: new information from the Indian Ocean and the Red Sea. Mar Biodivers 46, 483–487.
Sheather, S.J., 2004. Density estimation. Stat. Sci. 19, 588–597.
Stamatakis, A., 2014. RAxML version 8: a tool for phylogenetic analysis and post-analysis of large phylogenies. Bioinformatics 30, 1312–1313.
Stechow, E. & Müller, H.C., 1923. Hydroiden von den AruInseln. Abh. Senckenb. Naturforsch. Ges. 35, 459–478.
Stella, J.S., Pratchett, M.S., Hutchings, P.A. & Jones, G.P., 2011. Diversity, importance and vulnerability of coral-associated invertebrates. Oceanogr. Mar. Biol. 49, 43–116.
Swofford, D.L., 2003. PAUP. Phylogenetic Analysis Using Parsimony (and other methods). Version 4. Sinauer Associates, Sunderland, MA.
Talavera, G. & Castresana, J., 2007. Improvement of phylogenies after removing divergent and ambiguously aligned blocks from protein sequence alignments. Syst. Biol. 56, 564–577.
Tsang, L.M., Chu, K.H., Nozawa, Y. & Chan, B.K.K., 2014. Morphological and host specificity evolution in coral symbiont barnacles (Balanomorpha: Pyrgomatidae) inferred from a multi-locus phylogeny. Mol. Phylogenet. Evol. 77, 11–22.
Varela, C., 2012. Registros nuevos de hidrozoos (Cnidaria: Hydroidomedusae) para Cuba, con la descripción de una especie nueva. Solendon 10, 1–7.
Varela, C. & Cabrales Caballero, Y., 2010. Tres nuevos registros de hidrozoos (Cnidaria: Hydroidomedusae), para Cuba. Rev. Invest. Mar. 31, 104–105.
Vervoort, W, 1941. The Hydroida of the Snellius Expedition (Milleporidae and Stylasteridae excluded). Biological results of the Snellius Expedition XI. Temminckia 6, 186–240.
Villesen, P., 2007. FaBox: an online toolbox for fasta sequences. Mol. Ecol. Notes 7, 965–968.
Watson, J., 2005. Hydroids of the Archipelago of the Recherche and Esperance, Western Australia: Annotated list, redescription of species and description of new species. In: Wells, F.E., Walker, D.I. & Kendrick, G.A. (Eds.) The Marine Flora and Fauna of Esperance, Western Australia, pp. 495–612. Western Australian Museum, Perth, Australia.
Wickham, H., 2016. ggplot2: Elegant Graphics for Data Analysis. Springer-Verlag, New York, NY.
Williams, G.C. & Chen, J.Y., 2012. Resurrection of the octocorallian genus *Antillogorgia* for Caribbean species previously assigned to *Pseudopterogorgia*, and a taxonomic assessment of the relationship of these genera with *Leptogorgia* (Cnidaria, Anthozoa, Gorgoniidae). Zootaxa 3505, 39–5.
Wollschlager, J., Folino-Rorem, N. & Daly, M., 2013. Nematocysts of the invasive hydroid *Cordylophora caspia* (Cnidaria: Hydrozoa). Biol. Bull. 224, 99–109.
Yang, Z.H. & Rannala, B., 2010. Bayesian species delimitation using multilocus sequence data. Proc. Natl. Acad. Sci. USA 107, 9264–9269.

Supporting Information

Additional supporting information may be found online in the Supporting Information section at the end of the article.

Fig. S1. Phylogentic reconstructions based on the multi-locus dataset according to (a) Maximum parsimony, (b) Maximum likelihood, (c) Bayesian inference.

Fig. S2. Graphical evaluation of normality of residual to the fit of a linear model. QQ-plots (left) and dispersion diagram plots (right) for each cnidocyst type.

Fig. S3. Overview of the association between *Pteroclava krempfi* and alcyonancean octocorals.

Table S1. Table S1. Information on the specimens included in the analyses. Newly obtained sequences are in bold.

Table S2. Partitions and substitution models based on AIC for the multi-locus dataset.

Table S3. Support values for the clades recovered by single- and multi-locus analyses, based on maximum parsimony (MP), maximum likelihood (ML), Bayesian inference (BI). Highly supported nodes are in green (MP and ML bootstrap values ≥ 75, BI posterior probabilities ≥ 0.9).

Table S4. Genetic distances shown as % uncorrected p-distance ($\pm$ standard deviation) among and within cladocorynid species/clades.

Table S5. Outputs of the A11 BPP analyses based on different sets of priors and algorithms. Posterior probabilities (PP) are shown when > 0.

Table S6. Molecular diagnostic characters for each *Pteroclava krempfi* clade in the 3- and 5- species hypotheses for (a) 16S rRNA, (b) COX1, (c) COX3, (d) 18S rRNA, (e) 28S rRNA, (f) ITS, and (g) H3 markers. n.s. not sequenced.

Table S7. Measurements of cnidocyst length and width in *Pteroclava krempfi*.

Table S8. Descriptive statistical parameters of each *Pteroclava krempfi* cnidocyst type for clades Ia, IIa, III reported in μm as range (mean $\pm$ SD).

Table S9. Evaluation of the significance of the random effects by deleting one by one from the complete model.

Table S10. *Pteroclava krempfi* cnidocyst standard deviation (SD) of random effects from the best models.

File S1. R scripts used for the LMM and GLMM.